

**MASTER**

**Experimental Analysis of Carbon Dioxide Hydrogenation to Methanol and Di Methyl Ether (DME)**

Tadikamalla, N.

*Award date:*  
2021

[Link to publication](#)

**Disclaimer**

This document contains a student thesis (bachelor's or master's), as authored by a student at Eindhoven University of Technology. Student theses are made available in the TU/e repository upon obtaining the required degree. The grade received is not published on the document as presented in the repository. The required complexity or quality of research of student theses may vary by program, and the required minimum study period may vary in duration.

**General rights**

Copyright and moral rights for the publications made accessible in the public portal are retained by the authors and/or other copyright owners and it is a condition of accessing publications that users recognise and abide by the legal requirements associated with these rights.

- Users may download and print one copy of any publication from the public portal for the purpose of private study or research.
- You may not further distribute the material or use it for any profit-making activity or commercial gain



Department of Chemical Engineering and Chemistry  
Sustainable Process Engineering - Inorganic Membranes and Membrane Reactors

# Experimental Analysis of Carbon Dioxide Hydrogenation to Methanol and Di Methyl Ether (DME)

*Master Thesis*

Nithin Tadikamalla

Graduation Committee:

Prof.dr. Fausto Gallucci

Dr. Hamid Reza Godini

Dr. Luca De Felice

Prof.dr. Evgeny Rebrov

Eindhoven, March 2021



# Abstract

The efficient conversion of industrial scale generated carbon dioxide to valuable fuels or chemicals is evolving from being a promising alternative to becoming a necessity due to the ever tightening  $CO_2$  emission regulations. The ultimate goal is to approach a carbon-neutral energy efficient cycle.  $CO_2$  hydrogenation to Di Methyl Ether (DME) production can be identified as a distinguished green technology as its required hydrogen and Carbon dioxide can be provided by renewable sources and from the capture of  $CO_2$  emitted by the combustion chambers and chemical processing units. In addition, the DME that is produced can be used within the same industrial unit as a make-up fuel improving the overall environmental impacts.

$CO_2$  hydrogenation to methanol was carried out using catalysts synthesised via Co-Precipitation method and Precipitation Impregnation method. The catalytic performance of these catalysts were investigated and compared with benchmark commercial low pressure methanol synthesis catalyst. Subsequently, the better performing Co-Precipitation catalyst was introduced with DME catalyst (solid acid catalyst) to overcome the equilibrium constraints in the methanol synthesis. The methanol synthesis and methanol dehydration catalysts were combined and tested in a titanium fixed bed reactor to understand the influence of various bed configurations. The investigations explained the effect of spatial arrangement between the catalysts in macro scale. In addition, a dual catalyst was also tested and evaluated. Finally, the performance of the catalysts were studied by varying operating conditions such as temperature, pressure, GHSV, and  $CO_2/H_2$  ratio.

In the case of single catalysts, the catalyst synthesised via Co-Precipitation method has demonstrated a superior  $CO_2$  conversion and methanol yield when compared to the Precipitation Impregnation catalyst. Therefore, it is combined with methanol dehydration catalyst in various bed configurations consisting of 2 layer, 10 layer and physically mixed catalysts. The results obtained from these bed configurations showed that physically mixed catalyst where the active sites of both the catalysts are closer resulted in a higher combined yield of methanol and DME compared to other arrangements.

A Co-Impregnation (CI) dual catalyst synthesised with 2:1 ratio of HZSM-5 to methanol synthesis catalyst exhibited 14.5% yield of desired products (methanol and DME) at 260°C temperature, 15 bar pressure,  $CO_2/H_2$  ratio = 1:3.



# Contents

Contents	v
List of Figures	vii
List of Tables	ix
<b>1 Introduction</b>	<b>1</b>
1.1 Carbon dioxide emissions reduction	2
1.1.1 Carbon Capture and Storage	3
1.2 Carbon Capture Utilization	4
1.2.1 Direct use of $CO_2$	4
1.2.2 Conversion of $CO_2$	4
1.3 Thesis Objective	5
<b>2 Literature Survey</b>	<b>7</b>
2.1 Applications and Production	7
2.1.1 Methanol	7
2.1.2 Di Methyl Ether (DME)	8
2.2 Methanol Synthesis	8
2.2.1 Syngas Hydrogenation	8
2.3 $CO_2$ Hydrogenation	9
2.3.1 Reactions	9
2.3.2 Catalysts	10
2.3.3 Reactors	12
2.3.4 Operating conditions for $CO_2$ to Methanol and DME	13
2.3.5 Thermodynamic Calculation	13
<b>3 Experimentation</b>	<b>19</b>
3.1 Materials	19
3.1.1 Single Catalysts	19
3.1.2 Dual catalyst	20
3.1.3 Reagent gases and Auxiliary gas	20
3.2 Experimental setup	20
3.2.1 Feeding section	20
3.2.2 Reaction section	22
3.2.3 Analytics	23
3.2.4 Reactor automation	24
3.3 Methods	25
3.3.1 Catalyst Assembling	25
3.3.2 Catalyst Reduction	26
3.3.3 Reaction	26
3.4 Safety Aspects of the Experimental Setup	27

<b>4</b>	<b>Results and Discussion</b>	<b>29</b>
4.1	Catalytic performance of $CO_2$ Hydrogenation Catalyst . . . . .	29
4.1.1	Comparative Performance and Screening of the Catalysts . . . . .	29
4.1.2	Spatially arranged catalytic bed $CO_2$ to DME . . . . .	32
4.1.3	Performance of Dual Catalyst . . . . .	35
4.1.4	Sensitivity Analysis . . . . .	37
<b>5</b>	<b>Conclusions</b>	<b>39</b>
<b>6</b>	<b>Outlook</b>	<b>41</b>
	<b>Bibliography</b>	<b>45</b>
	<b>Appendix</b>	<b>51</b>
<b>A</b>	<b>Catalyst abbreviations, Composition</b>	<b>51</b>
<b>B</b>	<b>GC Calibration</b>	<b>52</b>
<b>C</b>	<b>Piping and Instrumentation Diagram (P&amp;ID)</b>	<b>56</b>
<b>D</b>	<b>Dual Catalyst</b>	<b>57</b>
D.0.1	Sensitivity analysis . . . . .	58

# List of Figures

1.1	<i>CO</i> <sub>2</sub> emissions emitted from each sector for selected regions [1]	2
1.2	<i>CO</i> <sub>2</sub> to valuable products using various conversion technologies[2]	5
1.3	Thesis Roadmap for this Research study	6
2.1	Applications of Methanol [3]	7
2.2	Types of catalysts used for <i>CO</i> <sub>2</sub> hydrogenation to methanol [4]	11
2.3	Predicted effect of temperature and pressure for <i>CO</i> <sub>2</sub> hydrogenation to methanol on <i>CO</i> <sub>2</sub> conversion based on thermodynamic calculations. Methane was not considered in the equilibrium conditions.	14
2.4	Predicted effect of temperature and pressure for <i>CO</i> <sub>2</sub> hydrogenation to methanol on methanol selectivity based on thermodynamic calculations . Methane was not considered in the equilibrium conditions.	15
2.5	Predicted effect of Feed ratio and temperature at 20 bar on <i>CO</i> <sub>2</sub> conversion for <i>CO</i> <sub>2</sub> hydrogenation to methanol based on thermodynamic calculations. Methane was not considered in the equilibrium conditions.	15
2.6	Predicted effect of temperature and pressure at <i>CO</i> <sub>2</sub> / <i>H</i> <sub>2</sub> ratio of 1:3 on <i>CO</i> <sub>2</sub> conversion based on thermodynamic calculations. Methane was not considered in the equilibrium conditions.	16
2.7	Predicted effect of temperature and pressure at <i>CO</i> <sub>2</sub> / <i>H</i> <sub>2</sub> ratio of 1:3 on methanol Selectivity based on thermodynamic calculations. Methane was not considered in the equilibrium conditions.	17
2.8	Predicted effect of temperature and pressure at <i>CO</i> <sub>2</sub> / <i>H</i> <sub>2</sub> ratio of 1:3 on DME selectivity based on thermodynamic calculations. Methane was not considered in the equilibrium conditions.	17
3.1	Schematic Representation of the experimental Setup	21
3.2	Tubular Furnace operated for providing heat to the titanium fixed bed reactor	22
3.3	Programmable Logic Controller (PLC) of the experimental setup	25
3.4	Methanol synthesis (single) catalyst arrangement inside the Titanium Reactor	26
3.5	Experimental Setup in the laboratory used for testing	27
4.1	Effect of temperature on <i>CO</i> <sub>2</sub> Conversion for single catalysts at 20 bar pressure and 400 <i>h</i> <sup>-1</sup>	30
4.2	Effect of temperature on methanol selectivity for single methanol synthesis catalysts at 20 bar pressure and 400 <i>h</i> <sup>-1</sup>	30
4.3	Effect of temperature on methanol yield for single catalysts at 20 bar pressure and 400 <i>h</i> <sup>-1</sup>	30
4.4	Effect of temperature on CO selectivity for single catalysts at 20 bar pressure and 400 <i>h</i> <sup>-1</sup>	30
4.5	Effect of Feed ratio on <i>CO</i> <sub>2</sub> conversion, methanol and CO selectivity for Co-Precipitation Catalyst. Reaction conditions: Pressure= 20 bar, GHSV = 400 <i>h</i> <sup>-1</sup>	31



LIST OF FIGURES

---

4.6	Different methods for combination of methanol synthesis catalyst with methanol to DME catalyst : Left) achieved by loading a layer of DME synthesis catalyst (pink) and a layer of methanol synthesis catalyst (blue) , Middle) achieved by loading multiple layers of methanol synthesis catalyst and Solid acid catalyst (10 layers), Right) Physical mixture of $CO_2$ to methanol catalyst with solid acid catalyst . . .	33
4.7	Combined methanol and DME selectivity for the tested bed configurations. Reaction conditions: $CO_2/H_2$ ratio =1:3, GHSV= $200 h^{-1}$ . unfilled circles (o) represents the tested reactor results . . . . .	34
4.8	Combined yield of methanol and DME for bed configurations containing methanol synthesis and methanol to DME catalysts. Reaction conditions: Pressure= 15 bar GHSV= $200 h^{-1}$ and $CO_2/H_2$ ratio = 1:3 . . . . .	35
4.9	Effect of temperature on $CO_2$ Conversion for a Co-Impregnation dual catalyst . .	35
4.10	Effect of temperature on Summation of methanol and DME yield . . . . .	35
4.11	$CO_2$ conversion and combined methanol and DME yield for a Co-Impregnated dual catalyst Reaction Conditions: Pressure = 15 bar , Temperature = $260^\circ C$ , $CO_2/H_2$ ratio =1:3 . . . . .	36
B.1	Schematic Representation of GC . . . . .	54
B.2	Calibration curves for gas components based on GC analysis . . . . .	55
C.1	Piping and Instrumentation Diagram(P&ID) of the experimental setup . . . . .	56
D.1	Effect of temperature on $CO_2$ Conversion an Selectivity of Methanol, DME, and CO	57

# List of Tables

3.1	Reagent gases and auxiliary gases used for experiments . . . . .	20
3.2	Dimensions of the Fixed Bed Reactor used for experimentation . . . . .	22
3.3	Lower and Upper Explosive Limits of Gases . . . . .	27
4.1	Results reported using Yates analysis showing the design of experiments used to identify the most significant parameter tested at constant pressure of 20bar * Detailed calculation is shown in the appendix D.1 . . . . .	37
A.1	Catalyst abbreviation used in this research study . . . . .	51
A.2	Composition by weight percentage present in the single catalysts . . . . .	51
A.3	Composition by weight percentage present in the dual catalysts . . . . .	51
B.1	Gas cylinders used for GC Calibration . . . . .	53
B.2	Characteristics of Compact GC . . . . .	53
D.1	Calculations reported for the dual Co-Impregnated Dual catalyst . . . . .	58
D.2	Analysis used for identifying the predominant parameter . . . . .	58
D.3	Nomenclature . . . . .	58



# Chapter 1

## Introduction

Over the past few years, the worldwide energy consumption has inclined as a result of population and economic growth. The global consumption of energy per hour is assumed to be approximately  $1.1 \times 10^{21}$  J by 2050 [5, 6]. Nowadays, the major sources of energy that is available globally are from fossil fuels i.e. crude oil, coal, and natural gas. The energy production from this fossil fuels accounts for two-thirds of greenhouse gases in which carbon dioxide is held as one of the most accountable one that causes global warming [7], climatic change [8], and ocean acidification [9].  $CO_2$  is a major anthropogenic green house gas that affects the radiative balance of the earth. In this concern, various global initiatives like the Intergovernmental Panel on Climate Change (IPCC) and the United Nations Climate Change Conference (UNCC) (COP21, Paris, 2015) have highlighted the urgency to mitigate  $CO_2$  emissions by at least by one half of the current value by 2050, aiming at limiting the global average temperature increase to a maximum of  $2^\circ C$  to avoid more threatening consequences [10].

Carbon dioxide has steadily increased after the pre-industrial era and reached 35.9 Gt in 2014 which shows that  $CO_2$  was present in large form of carbon resource [11]. The total primary energy supply has increased by 150% from 1971 to 2013 globally due to the increasing worldwide energy demand for the development and economic growth [12]. Although, there exists tremendous developments in nuclear and renewable energy sector over the last few decades, fossil fuels remain the world's primary energy supply, steadily contributing to  $CO_2$  emissions. Moreover, these  $CO_2$  emissions have significant effect on the ocean environment. The pH value of the ocean decreases when  $CO_2$  is added into it [13]. The sea water gets acidified creating potential detrimental effects on marine life [8, 14]. Therefore, the urge to develop technological processes to abate these  $CO_2$  emissions associated with the use of these fossil fuels that has to include the capture and subsequent valorization of the  $CO_2$  produced.

The global emissions of  $CO_2$  can be determined by three crucial factors namely, the geopolitical location of the region or country, economy and type of fuel used to produce the energy. The major carbon dioxide producing countries in the world are China, USA, India, Russia, Japan, Germany, Iran, South Korea, Canada, and Saudi Arabia. According to of International Energy Agency (IEA), in 2016 approximately a quarter of global carbon dioxide emissions were produced in Asia from heat generation and electricity [From figure 1.1] [1].  $CO_2$  is emitted by a large variety of sources ranging from large scale to small scale industries. Power plants, petroleum, chemical, steel and cement industries, are major large scale industries, while small scale industries like industrial and commercial buildings and transportation add to the emissions [15]. In power-plants and other industries, most of the  $CO_2$  emissions occurs due to burning of the coal. Hence, various strategies or methods are required for abatement of carbon dioxide.

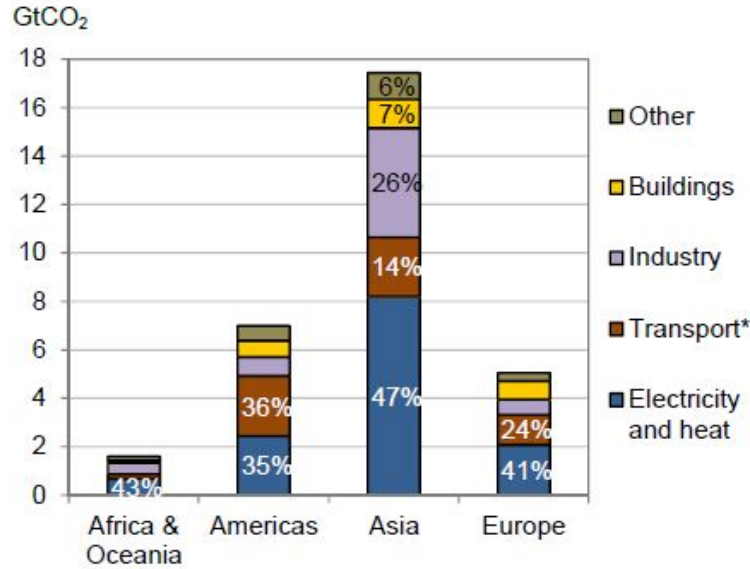


Figure 1.1:  $CO_2$  emissions emitted from each sector for selected regions [1]

## 1.1 Carbon dioxide emissions reduction

Many research activities are concentrated on reducing the carbon dioxide emissions, especially in transportation and energy sector as well as using the carbon dioxide that is already available for conversion to profitable products. The strategies for abatement of the carbon dioxide are mentioned as follows:

- 1) Shifting from fossil fuels to renewable energy sources
- 2) Improving the technologies in the industries and power sectors
- 3) Replacing the coal fired units with natural gas units
- 4) Carbon capture Storage (CCS)
- 5) Carbon Capture Utilisation (CCU)

Replacing/Substituting fossil fuels with renewable energy sources is still in a primary stage. A recent study conducted by an institute related to the long-term electricity which planned to substitute fossil fuels with renewable energy resources exhibited promising results[16]. However, this would take a lot of time and research to bring it into existence for industrial applications. Industries and power sectors can utilise the nuclear energy to produce the required electricity. Nevertheless, they had to take numerous steps and safety measures in order to implement nuclear energy in industries. Moreover, a nuclear plant has many legal complications in a few countries [17]. Natural gas fired power plants produce nearly half the  $CO_2$  compared to coal fired power plants; replacing the coal fired units with natural gas units leads to lower emissions [18]. Nonetheless, substituting coal fired plants with natural gas fired plants requires extensive modifications to existing power plant equipment including the internal structure of the boiler. As shifting from fossil fuels or improving the technology in power plant or replacing a coal fired units with natural

gas units that were described above take a lot of time or research for industrial applications. They do not contribute to the  $CO_2$  emissions abatement at the current stage or situation. Thus, a successful and strong strategy is required for lowering  $CO_2$ . In this case, Carbon Capture and Storage (CCS) and Carbon Capture and Utilisation have been extensively researched and are capable of controlling the  $CO_2$  emissions practically.

### 1.1.1 Carbon Capture and Storage

Carbon dioxide capture and storage is considered as one of the most crucial and valuable technologies in reduction of  $CO_2$  emissions over the last decades. The capture of the carbon dioxide and the efficiency of the carbon capture methods extracting  $CO_2$  from different sources will play a role in valorizing the alternative carbon feed stock. This Carbon Capture and Storage (CCS) technology involves  $CO_2$  separation from flue gases from the major carbon dioxide emission industries and power plants. Typically, around 85% to 90% of Carbon dioxide is captured with these technologies. In general,  $CO_2$  is separated in three ways and they are described briefly as shown below. Besides capturing the carbon dioxide it is also important to understand the costs involved.

- 1) Pre-combustion
- 2) Post Combustion
- 3) Oxy-fuel combustion

#### Pre-combustion

Pre-combustion technology separates  $CO_2$  prior to the combustion in an energy plant. This process leads to cleaner products in combustion process as the  $CO_2$  is eliminated in the beginning. Therefore,  $CO_2$  emissions reduces in the atmosphere. It is likely to implement this kind of a process in a new power plant as it is quite expensive to modify the existing ones[19]. The overall costs related to the current Pre-combustion capture technologies are approximately 60\$/ton  $CO_2$ . The performance requirements for Pre-combustion of  $CO_2$  was researched by Ku et al with a single step high temperature membrane process [20]. It was reported that a high performance membrane can deliver 90% carbon capture at price below 20\$/ton  $CO_2$  [21].

#### Post combustion

Post combustion technology captures the  $CO_2$  at the end of the combustion process. The hot combustion gases exiting the boiler contains nitrogen from air along with water vapor in lower concentrations along with  $CO_2$  that is based on the combustible gas used. In addition, air pollutants such as sulfur dioxide, particulate matter are removed. The main challenges faced in a post combustion process are the low partial pressure of  $CO_2$  and processing the enormous amount of flue gas [22]. This technology can be adapted for both new and old power plants as it requires an additional  $CO_2$  separation unit to be installed after the combustion process to reduce the carbon dioxide emissions.

#### Oxy-fuel Combustion

Oxy-fuel combustion is a process of burning the fuel with pure oxygen for combustion rather than air as the primary oxidant which results flue gas consisting of water vapor and carbon dioxide. This reduces the formation of nitrogen oxides, so that the exhaust gas is essentially  $CO_2$  after condensing the water which results in removing the  $CO_2$  to separate easily. By using this process, roughly 75% less flue gas than air fueled combustion [23]. However, it has a major energy penalty while withstanding the higher combustion temperatures during the production of pure oxygen by air separation and on the manufacture of the required materials. The thermodynamic energy

demand that is essential for capturing 90% of the  $CO_2$  is from the flue gases of a coal-fired power plant and it is reported to be around 3.5% with flue gas composition of  $CO_2$  being 12-15% [24]. The separated  $CO_2$  is either stored in the underground at specified locations or it is transported and used for various purposes. The cost of using this captured carbon-dioxide as a valuable feedstock will depend on the implementation of government and industrial driven policies for instance Levelised Cost of Energy (LCOE) in Europe [25].

## 1.2 Carbon Capture Utilization

In a Carbon Capture Utilization,  $CO_2$  is used for making value added products instead of storing it. Carbon dioxide Utilization can be classified mainly into two categories namely direct use of  $CO_2$  and conversion of  $CO_2$ . The objectives of research and development efforts on  $CO_2$  conversion and utilization can incorporate one or more goals as listed below depending on the applications [26].

- 1) To make use of  $CO_2$  for environmental-benign physical or chemical process depending on the special characteristics of  $CO_2$ .
- 2) To produce valuable materials and chemicals by making use of  $CO_2$ .
- 3) To recycle  $CO_2$  as a carbon source for fuels and chemicals.
- 4) To replace a hazardous substance or a less-effective substance in existing process with  $CO_2$  as an alternate medium or co-reactant or solvent.

### 1.2.1 Direct use of $CO_2$

The direct use of  $CO_2$  includes Enhanced Oil Recovery (EOR), fire suppression, industrial uses, refrigerant fluids, food processing and preservation industries etc. Carbonation of  $CO_2$  in the beverage industry involves injecting  $CO_2$  into cold drinks, sparkling water, etc. The super-critical pressurised  $CO_2$  is used for extraction of fragrances and essences from plants or fatty acids or proteins and hydrocarbons from algae.  $CO_2$  can also be used as a cleaning agent. It is used for cleaning circuit boards, semiconductor devices etc. In mechanical industries, the usage of  $CO_2$  is observed in moulding, cutting and soldering [27].

Although, direct use of  $CO_2$  has wide range of applications in industries. Nevertheless, their market scales are small and hence generates a very small impact on the overall  $CO_2$  emission [2]. This might be a better option compared to others, but not the best option to reduce the  $CO_2$  that is present currently.

### 1.2.2 Conversion of $CO_2$

As mentioned in the previous subsection 1.2.1, there are various way to utilize Carbon dioxide. However, it is very less compared to the  $CO_2$  conversion. The conversion of  $CO_2$  to profitable products is an outstanding option toward sustainable carbon cycle. The  $CO_2$  can be converted to various valuable products as shown in below Figure 1.2 through numerous methods. For instance, thermochemical, electrochemical, photo- catalytic and photo-electrochemical [2].

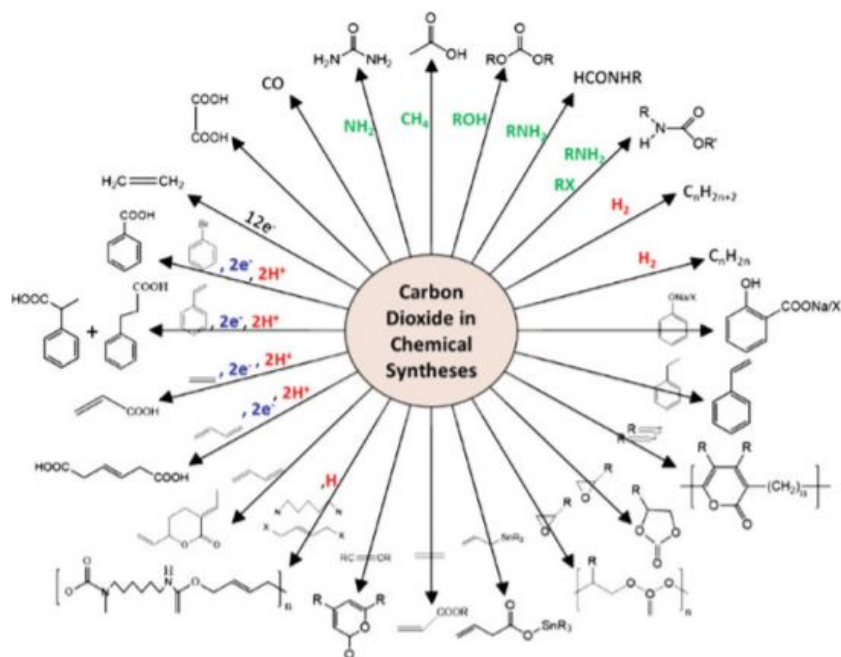


Figure 1.2:  $CO_2$  to valuable products using various conversion technologies[2]

Utilizing  $CO_2$  as a valuable feed stock to obtain profitable products has been the objective of many scientists and in return it reduces the dependence on fossil fuels. Research studies pioneered towards converting  $CO_2$  to  $C_1$  building block chemicals and has already made noteworthy achievements [28]. Methanol is among the most highly used  $C_1$  chemicals with applications ranging from fuel cells to being an excellent blend for internal combustion engines [29]. It is found to be a very important industrial commodity chemical with a global production of 110 million metric tons [30]. Moreover, the conversion of this methanol to DME also has a strong potential in reducing the  $CO_2$  in a short time span. In 2.1, methanol and DME production along with their applications and synthesis procedures is described in detail.

### 1.3 Thesis Objective

In this thesis, the main objectives are

1. To study the effects of the reactor bed configurations in macro scale.
2. To investigate the performance of the single and dual catalyst at various operating conditions.

From the view of thermodynamics, the yield of methanol synthesis is limited by equilibrium constraints which can be seen in the equation 2.5. To overcome this limitations, a strategy was applied by introducing an additional catalyst in order to enable an auxiliary reaction to shift the equilibrium towards valuable and profitable products. In this research study, spatially patterned such as 2 layered catalyst, 10 layered catalyst or physically mixed catalyst were tested. Essentially, a 2 layered catalyst is placing the  $CO_2$  to methanol catalyst next to DME catalyst. For a 10 layered catalyst, the methanol catalyst and DME catalyst are placed subsequent to each other continuously for 10 sets. In case of physical mixing, both the methanol synthesis catalyst and DME catalyst are assorted. The effect of the described bed configurations are studied in macro scale. The combined Selectivity and yield of methanol and DME for these spatially arranged catalysts or physically mixed catalysts bed were compared and evaluated.



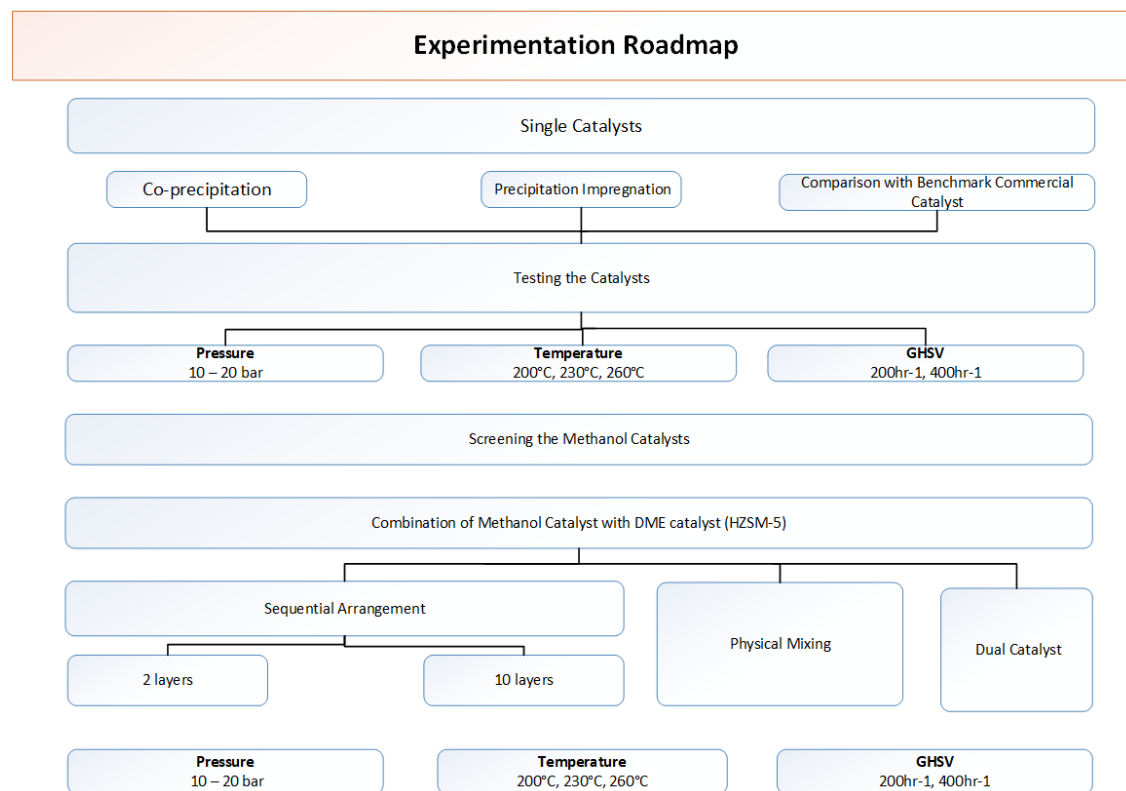


Figure 1.3: Thesis Roadmap for this Research study

A detailed thesis road map for this research is shown in the Figure 1.3. Experimental tests of  $CO_2$  hydrogenation to methanol and later to DME were performed in the titanium reactor in order to compare the performance of various single catalysts synthesised via different methods and dual catalyst.

In the first step, the methanol synthesis catalysts synthesised via Co-Precipitation and Precipitation Impregnation methods along with the commercial Low Pressure methanol catalyst were tested at highest pressure in the experimental setup (i.e 20 bar) with varying temperature from 200°C to 260°C. The main intention was to screen the performance of the single catalysts.

In the next step, the best performing catalyst in the above step was chosen to be tested along with HZSM-5 catalyst for methanol dehydration in the titanium bed reactor in various bed configurations such as 2 layer, 10 layer, and physical mixing as shown in the figure 4.6. The main intention or goal was to track the methanol produced and consumed due to the spatial arrangement between catalysts in macro scale under various temperatures and pressure.

In the final step, the performance of a synthesised Co-Impregnated dual catalyst consisting active sites of methanol dehydration and methanol synthesis in a single catalyst with weight percentage of 2:1 was tested. Furthermore, the predominant parameter influencing the performance of this dual catalyst was also studied via experiments designed using Yates table.

## Chapter 2

# Literature Survey

## 2.1 Applications and Production

### 2.1.1 Methanol

Methanol is the simplest alcohol that is one of the crucial bulk commodity or feed-stock for the chemical industry and fuel industry. It can be used as initial feed for producing larger chemicals. It is a colorless polar liquid which is miscible in water at room temperature, that is highly toxic for humans and flammable in nature [31]. Methanol has a higher energetic efficiency than its derivatives.

In 2011, 53 million tonnes of methanol were sold, whereas in the year 2015 the demand and usage of methanol increased and reached 75 million metric tonnes per year. Currently, the methanol plants that were installed worldwide have a production of 110 million metric tons to meet the methanol demand[30]. The towering demand for methanol globally is due to the growth of the Asian market. This demand has increased by 500% over the last 15 years. Methanol has a wide range of applications and is used in the polymer industry, pharmaceutical applications and organic synthesis [32]. In particular, a major part of the methanol produced globally is consumed for production of acetic acid, methyl and vinyl acetates, methyl methacrylate, methyl terbutyl ether (MTBE), fuel additives and the rest is employed in the synthesis of formaldehyde as shown in Fig 2.1.

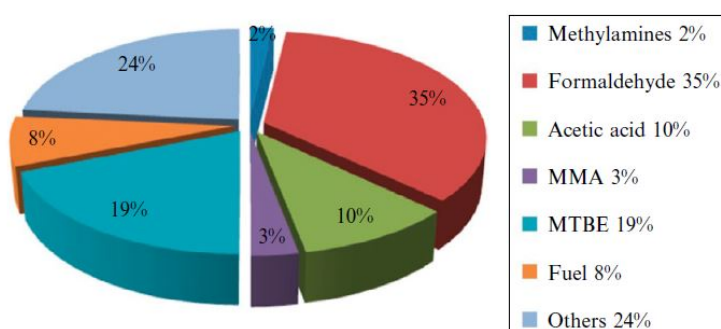


Figure 2.1: Applications of Methanol [3]

### 2.1.2 Di Methyl Ether (DME)

Di Methyl Ether(DME) which is also known as Methoxymethane ( $CH_3OCH_3$ ) is a colorless gas that is used as a coolant and propellant. Since, DME has C-O, C-H bonds and no C-C bonds it results in less emissions of carbon monoxide and other unburned hydrocarbons during combustion. DME can be used as pesticide, polishing agent and anti rusting agent. In addition, DME being a potential diesel substitute has attracted several researchers [33, 34, 35]. Due to its high cetane number (55-60) and its excellent properties, it is also considered as an better alternative to the present transportation fuel. Moreover, it is widely recommended as environmentally friendly aerosol and green refrigerant [35].

The DME demand is anticipated to increase above 7 million metric tons/year by 2015 while the global capacity is between 10 to 12 million metric tons/year . DME has a huge demand and commercial production in Asia due to the use of domestic fuel and growing demand in the automobile industry. China is considered as the highest producer and consumer of DME with capacity around 200,000 metric tons per year reported [36]. In November 2020, the price of DME (99% or above) in China has reached 2,830 RMB/ton which corresponds to €355.78/ton [37].

Currently, there exist two steps to produce DME using  $CO_2$  and  $H_2$  as feed components: a single step process, two step process. The two step process involves methanol synthesis followed by a dehydration step to DME. In a single step process the synthesis of methanol and dehydration to DME is combined in one reactor [38, 39].

The demand, production and applications of methanol and DME has also motivated to further research in detail regarding the routes of methanol and DME synthesis.

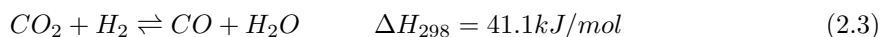
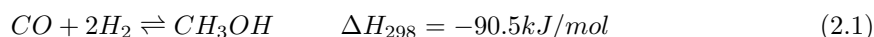
## 2.2 Methanol Synthesis

Methanol can be produced/synthesised from two routes, either via syngas or  $CO_2$  hydrogenation. Both these routes are mentioned in detail below:

### 2.2.1 Syngas Hydrogenation

Methanol which is also coined as the wood spirit was produced by heating of the wood in anaerobic conditions before the modern industrial era. The wood distillation process produced an extract with contaminants along with methyl alcohol. The process was improved by Robert Boyle by purifying the extract using a reaction with milk and termed it as wood vinegar. Due to contaminants, the yield obtained was too low. To improve the yield, numerous metals and oxides were tested. In 1927, the development staged process was turned to the production stage and exported[3]. In 1960, Imperial Chemical Industries (ICI) produced a low-pressure method (35-40 bar) at 200°C - 300°C. This method included a highly selective copper-based catalyst along with an advanced purification process for synthesis gas which was free from sulphur and carbonyl contaminants [40].

In general, syngas can be produced from various sources like natural gas, gasification or partial oxidation of coal, shale gas, and biomass. The relevant reactions for the production of methanol from synthesis gas are shown below:



Methanol is formed using syngas in the operating temperatures of 250°C - 300°C, and a pressure of 50-100 bar with Stoichiometric number slightly above 2 over a Copper-Zinc Oxide catalyst with Aluminium Oxide [41]. From the reactions mentioned above it can be seen that the production of methanol is exothermic in nature and involves reduction of amount of molecules present. According to the Le Chatlier's principle the productivity can be increased by increasing pressure and reducing temperature.

$$SN = \frac{y_{H_2} - y_{CO_2}}{y_{CO} + y_{CO_2}} \quad (2.4)$$

In the above equation,  $y$  denotes the partial pressure of the gas components according to the subscript notation. The desired SN (stoichiometric number) in the feed is equal to 2.  $SN > 2$  specifies an excess of hydrogen whereas  $SN < 2$  specifies a carbon rich feed mixture.

## 2.3 $CO_2$ Hydrogenation

$CO_2$  is very stable linear molecule. A catalyst with high stability, optimized reaction conditions and a substantial energy input are required for converting  $CO_2$  into value-added chemicals[3]. Using  $CO_2$  as a feed stock has various advantages. It is inexpensive, abundant, non corrosive, nontoxic, non flammable, and easy to store. Methanol production from  $CO_2$  is favourable not only for the use of non-fossil fuel resources, but also it consequently closes the carbon cycle[42]. Therefore, it has gained a lot of researchers attention recently, as it provides an alternative for industrial syngas hydrogenation process.

Carbon Recycling International (CRI) has been the world leader in producing methanol from  $CO_2$  which is extracted from waste gas streams and hydrogen which is generated from water electrolysis using renewable power. The plant has a production capacity of 50,000 - 100,000 ton/year of methanol. Conventional methanol production plants produces 0.7 ton of  $CO_2$  per ton of methanol from natural gas reforming while over 3 ton of  $CO_2$  per ton of methanol using coal gasification. In contrast, CRI's demonstration plant in Svartsengi (Iceland) which is named after George Olah, consumes more than 1.3 ton of  $CO_2$  for every 1 ton of methanol produced. This reveals Carbon dioxide valorization to methanol has the potential to reduce the concentration of the  $CO_2$  in the atmosphere[43]. In addition, another demonstration plant in Japan constructed by Mitsui Corporation produced methanol from  $CO_2$  hydrogenation. They have also used the  $CO_2$  that was extracted from industrial waste gas streams and hydrogen produced from the photocatalytic water splitting. In 2008, a pilot plant was built in Osaka, Japan. This pilot plant produced around 100 tonnes/year of methanol using Cu ZnO based catalyst in a fixed bed reactor [44].

### 2.3.1 Reactions

#### $CO_2$ hydrogenation

In the process of DME production. DME can be synthesised in two following methods:

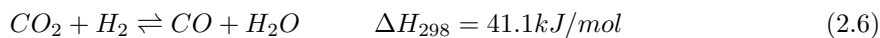
1. Indirect synthesis
2. Direct synthesis

The indirect synthesis method is a two step process. The reactions for an indirect synthesis route of DME can be written as follows.

Initially,  $CO_2$  is converted to methanol :



Considering the Reverse Water Gas Shift reaction (RWGS) :



DME being produced by the dehydration of methanol according to the following reaction:



For a single step process/ Direct method, the  $CO_2$  hydrogenation, methanol dehydration and reverse water-gas shift reactions are put together and the overall reaction can be expressed as:



### 2.3.2 Catalysts

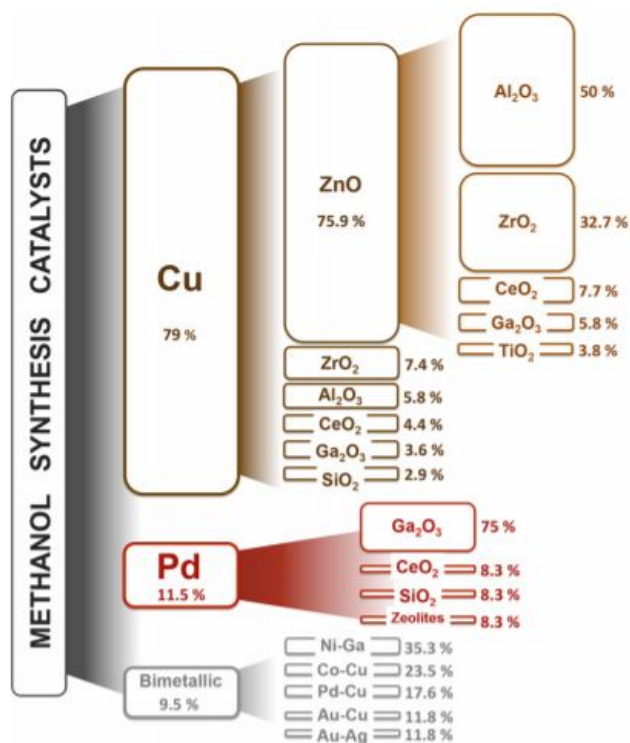
For a  $CO_2$  to DME process, the catalyst of methanol synthesis has to be efficient in order to produce higher amount of methanol which converts to DME in the presence of methanol dehydration catalyst. An extensive research has been performed on finding the better catalysts for  $CO_2$  to DME.

#### Catalysts for Methanol Synthesis

The first and foremost catalyst used for the methanol synthesis process is ZnO on  $Cr_2O_3$ . In 1966, copper based catalysts were introduced for synthesis of methanol. The elemental copper cannot be directly used as the methanol synthesis catalysts due to its poor thermal stability. Various studies related to the single crystal and poly-crystalline copper showed high activity towards the formation of methanol [45]. The role of copper as an active catalyst part for  $CO_2$  hydrogenation to methanol has been investigated for decades [46, 47]. In the past 10 years, 79% of the reports published in the field of  $CO_2$  hydrogenation to methanol described catalysts based on copper. The specific surface area of copper and the particle size of copper are some of the predominant factors which affect the catalytic performance. The smaller particle size has higher dispersion and lowers the agglomeration which in return enhances the catalytic activity.

The metal oxides such as Zr, Ce, ZnO, Cr as shown in the figure 2.2 are added to stabilize copper. The ZnO supported catalyst is the most extensively used due to its high activity. Moreover, ZnO present in the catalyst plays a pivotal role in maintaining a strong metal support interaction with Cu species that leads to formation of methanol [48]. However, excess of Zn has a negative effect on activity of the catalyst.

H. R. Godini et al. reported and summarised various researches that were conducted since 1980 in the field of  $CO_2$  hydrogenation to methanol, especially under low to medium operating pressure of upto 20 bar [49]. Several research groups have discovered that Cu/Zn based catalysts with high copper dispersion characteristic displays better performance. Along with the metal and support material combination, the synthesis method also plays a vital role. Typically, the Cu-ZnO catalysts or Cu-ZnO/promoter catalysts that are commercially available were synthesised using Co-Precipitation method using 50-70 mol % of CuO, 20-50% ZnO, and 5-20 %  $Al_2O_3$  [4, 24]. The catalyst composition and catalyst preparation methods along with its conditions have high influence on the surface structure of catalysts [50]. Besides Co-Precipitation method and other various methods such as Precipitation Impregnation method are used in the literature for better yields [49]. Therefore, these synthesis procedures are followed for preparation of the methanol synthesis catalyst. A comparative examination of these catalysts performance was carried out for the case of  $CO_2$  hydrogenation to methanol.

Figure 2.2: Types of catalysts used for  $CO_2$  hydrogenation to methanol [4]

### Catalysts for Methanol Dehydration

Di methyl ether is produced through methanol dehydration step over solid acid catalyst.



The methanol dehydration is an exothermic reversible reaction. The number of moles are equal on the both side of the reaction. Thus, the reaction pressure doesn't have an effect on the  $CO_2$  conversion. However, the reaction temperature has shown to have a thermodynamic benefit for the DME production.

The active sites required for methanol dehydration to DME are called as acid sites. Various solid acid catalysts have been investigated for methanol dehydration reaction. Solid acid catalysts such as  $\gamma-Al_2O_3$  and the modifications of alumina with  $TiO_2$ -  $ZrO_2$ ,  $SiO_2$ , ion exchange resins and zeolites HZSM-5 etc [35]. Among these, HZSM-5,  $\gamma-Al_2O_3$  are the most extensively studied solid acid catalysts for dehydration to DME. The major reasons for choosing  $\gamma-Al_2O_3$  as the methanol dehydration catalyst is due to its high specific area and good thermal and mechanical stabilities, acid base properties and a high selectivity towards DME formation [35]. Later, various modifications were made on this  $\gamma-Al_2O_3$ . It was also noticed that the sulfate treatment lead to increase in the  $\gamma-Al_2O_3$  acidity. Few researchers have investigated silica-modified  $\gamma-Al_2O_3$  and reported that it performs better than the unmodified  $\gamma-Al_2O_3$  [51].

Although the  $\gamma-Al_2O_3$  was investigated deeply for methanol to DME, it still posses few drawbacks for this reaction. The acid sites that were present on the  $\gamma-Al_2O_3$  are mainly Lewis acid type [52]. The water that is produced during the reaction strongly adsorbed on the Lewis acid sites of  $\gamma-Al_2O_3$ . Therefore, it will decrease the performance of the methanol dehydration. In addition it will inhibit the DME formation [53].

HZSM-5 offers higher activity compared to  $\gamma\text{-Al}_2\text{O}_3$  at relatively low temperature range i.e 240°C to 280°C. HZSM-5 is thermodynamically more favourable when compared to  $\gamma\text{-Al}_2\text{O}_3$  [54]. During the methanol dehydration, water is produced as mentioned in the equation 2.9. Moreover, HZSM-5 has higher resistance towards water than  $\gamma\text{-Al}_2\text{O}_3$  [55].

### Catalyst arrangements for $\text{CO}_2$ hydrogenation to DME

As per equation 2.5, the synthesis of methanol has thermodynamic equilibrium constraints. To overcome these limitations, a methanol dehydration catalyst is introduced next to methanol synthesis catalyst i.e. in layered manner to produce DME in a single step. Because of this consecutive nature of DME formation, the thermodynamic aspects can be mitigated. The methanol that is produced from the methanol synthesis catalyst is converted to DME via Methanol Dehydration catalyst. In the literature very few researchers have studied the effect of spatially arranged or layered catalysts. McBride et al. have simulated this arrangement with increasing the number of layers from 2 layers to 40 layers. The increase in DME productivity was observed with infinite number of layers. In addition, they have compared the arrangements of the catalysts to a cascade model of two step process [56].

Another possibility for producing the DME in a single step can be a physical mixture of the catalysts assumed as infinite layers where the methanol synthesis and methanol dehydration catalysts are mixed together before placing in the reactor. Bonura et al. have studied the effect of the catalyst arrangements using four different combination methods of methanol synthesis catalysts with methanol dehydration catalyst in a fixed bed stainless steel reactor at 443K to 563K, and pressure ranging from 10 bar to 50 bar. Their study has reported that a bi-functional catalyst prepared by physical mixing exhibits a superiority in performance when compared to the other configurations [57]. Besides, a study performed by Ren et al. reported the effect of the mixing methods of the both catalysts for  $\text{CO}_2$  hydrogenation to DME and concluded that mixing of the pelletized catalyst had better stability and reduced Cu oxidation [58]. Therefore, these bed configurations have been decided for being tested in the fixed bed reactor and the effect of these beds are examined and compared in the results section.

### Dual Catalyst for $\text{CO}_2$ hydrogenation to DME

An additional case that can be considered to overcome the thermodynamic equilibrium constraints of methanol is a dual catalyst. Using a dual catalyst, the methanol which is produced is continually removed from the reaction mixture and is converted to DME in a single reactor. A dual catalyst requires two types of active sites, one is for the methanol formation and the other one is for the methanol dehydration. The dual catalyst has to have a good intimate contact between these two functions. Frusteri et al. investigated the acid sites for  $\text{CO}_2$  to DME using CuZnZr-MFI catalyst and reported that the active sites can be maximised by using Co-Precipitation of CuZnZr methanol synthesis precursors [59]. Besides, Bonura et al investigated CuZnZr/ferrite catalysts using various synthesis procedures for the case of  $\text{CO}_2$  to DME hydrogenation reaction. Their study has revealed that catalyst prepared via Co-Precipitation has resulted highest  $\text{CO}_2$  conversion of 23.6% at 260°C and a combined Methanol/DME yield of 15%. In addition, they have concluded that the active sites distribution affects the performance of catalyst significantly [60].

Apart from the catalysts, a reactor also plays a major role in identifying the performance of the catalysts. The study regarding the reactors from the literature is presented in the next section.

## 2.3.3 Reactors

In general, a reactor can be defined as a device which encloses the catalyst and reaction medium. Reactor is used as a container where the reactants are fed into the system at particular reaction

condition for specific amount of time. Thus, a reactor provides a control of various reaction conditions such as the temperature and pressure. In addition, the pinch analysis also plays a role while focusing on the reactors. It helps in designing a process by minimizing the energy consumption and maximizing the energy efficiency. For the case of the Carbon-dioxide to methanol few advancements in the reactor aspects were observed in the literature.

Researchers have investigated  $CO_2$  hydrogenation to methanol with micro reactors. Liang et al. has reported 9.9 % of  $CO_2$  conversion and 82.17 % selectivity of methanol under 30 bar pressure at 250°C [49, 61]. Besides, F.Gallucci et al. have investigated the possibility of  $CO_2$  hydrogenation to methanol via a zeolite membrane reactor and separated products from the catalytic reaction system [62]. They have studied the membrane reactor for  $H_2/CO_2 = 3$  and 7 ratios. In general, fixed bed reactors are used for gas phase reactions. It has unique advantages when compared to other reactors for  $CO_2$  hydrogenation to methanol. A higher conversion of  $CO_2$  and selectivity of methanol was reported by Cai et al. in their study while using a fixed bed reactor [63]. Similarly, Jalama et al. reported 29.2% yield and 31.7% selectivity of methanol using a fixed bed reactor at higher pressure (i.e 110 bar) [64].

Although there are some advancements in the type of reactors, a fixed bed reactor was found to be the most extensively used reactor in the literature for testing the catalysts in a standard manner with co-feeding of the reactants. Moreover, for the case of  $CO_2$  to DME, the testing of spatial arrangement of the two catalysts is more convenient in a fixed bed reactor compared to other reactors.

### 2.3.4 Operating conditions for $CO_2$ to Methanol and DME

The  $CO_2$  hydrogenation to methanol as mentioned in the equation 2.5 shows that it is an exothermic reaction and a lower temperature is favoured. The temperature range targeted for methanol synthesis using Copper based catalyst is 200° to 260° [49], [65]. Higher pressures are favoured for the methanol synthesis reaction as per Le Chatelier principle. It was found that the copper based catalyst was tested upto 442 bar [66].

In particular, the hydrogenation of carbon dioxide to DME has been investigated at the temperatures ranging from 200°C to 275°C and pressure from 2.0 MPa to 5.0 MPa. The study by Erena et al. have reported that the optimum temperature is 275°C for maximising the yield of DME [67]. However, another research group have investigated the DME production from  $CO_2$  in wide range of temperature ranging from 232°C to 262°C and found that the DME selectivity to be maximum at 262°C. [68].

The effect of pressure for  $CO_2$  hydrogenation to DME has been studied in the range of 2.0 MPa to 5.0 MPa with regards to the product selectivity and catalyst activity. Erena et al. have reported that the optimum pressure was 4.0 MPa for maximum  $CO_2$  conversion and yields of the desired products (methanol and DME) [67]. However, another group has reported decrease in the  $CO_2$  Conversion and DME selectivity while the pressure was increased from 3.0 MPa to 4.0 MPa [69].

Increasing the pressure of the gas streams to a higher level and processing them are very expensive. Hence, a pressure of upto 20 bar is considered for this research in the techno economic point of view.

Although the operating conditions vary based on the catalyst. The main purpose is to observe the range of temperature and pressure associated for the  $CO_2$  hydrogenation to methanol and DME.

### 2.3.5 Thermodynamic Calculation

The energy minimization technique is used to analyze the equilibrium composition in the non-stoichiometric systems. The variables that are present are pressure and temperature, hence a



gibbs free energy minimization approach was selected. For the thermodynamic analysis of this system, a RGibbs reactor model in Aspen was used. Due to existence of non-ideal behaviour, the Soave-Redlich-Kwong (SRK) model present was chosen as the equation of state [70]. The estimated equilibrium conversion at 250°C and 5 MPa obtained for this model is in line with the reported values in literature for instance by F.Gallucci et al [62].

### $CO_2$ to Methanol

The reactants and products in the system are taken into account. For the case of methanol,  $CO_2$ ,  $CO$ ,  $H_2$ ,  $H_2O$ ,  $CH_3OH$  components were taken into account for the thermodynamic calculation. The plots that are reported here are considered for the temperatures 200°C to 260°C at which the experimentation is targetted. In addition, temperature 290°C is chosen to be reported to observe the trend.

### Effect of Temperature and Pressure

The impact of the temperature and pressure on  $CO_2$  conversion can be seen in the figure 2.3. It can be observed from the figure that at the lowest temperature i.e. 200°C and highest pressure (20 bar) , a highest  $CO_2$  conversion is observed for the methanol synthesis. As the temperature is increased beyond 290°C, the selectivity of CO increases as the RWGS reaction is endothermic as described in Eqn 2.6 which is competitive and dominates the process. Figure 2.4 illustrates that as the temperature increases the methanol selectivity decreases. With regards to pressure, increase in the pressure has increased the methanol selectivity. It can be concluded that at the equilibrium conditions, the carbon-dioxide conversion and selectivity of methanol increases while the pressure is increased.

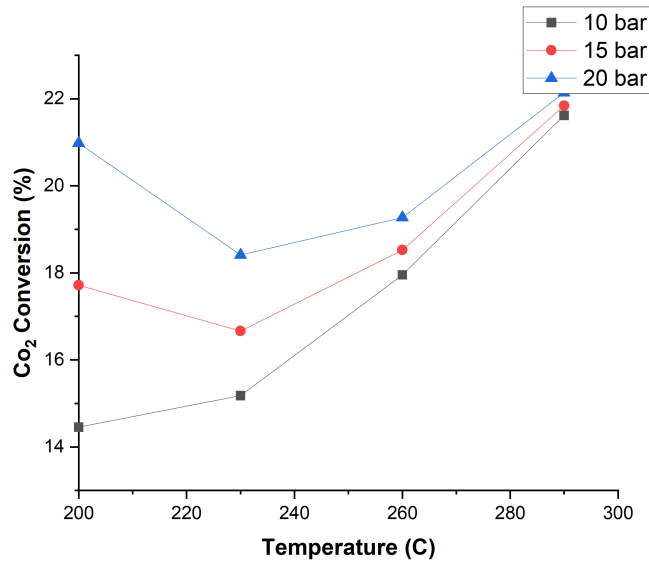


Figure 2.3: Predicted effect of temperature and pressure for  $CO_2$  hydrogenation to methanol on  $CO_2$  conversion based on thermodynamic calculations. Methane was not considered in the equilibrium conditions.

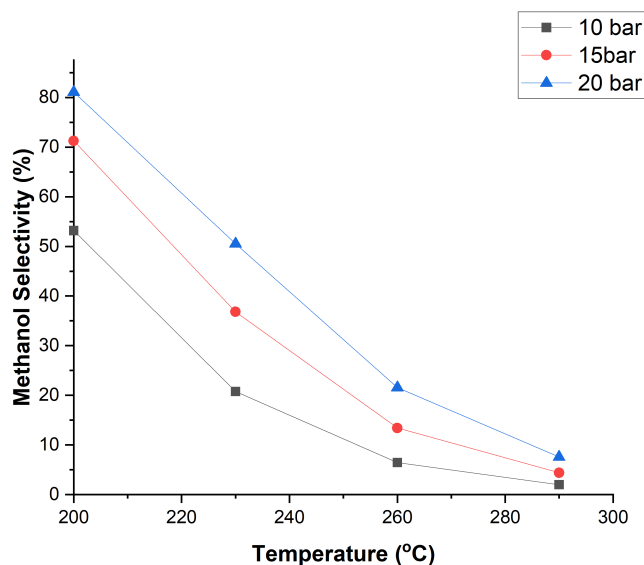


Figure 2.4: Predicted effect of temperature and pressure for  $CO_2$  hydrogenation to methanol on methanol selectivity based on thermodynamic calculations. Methane was not considered in the equilibrium conditions.

#### Effect of $CO_2/H_2$ molar ratio

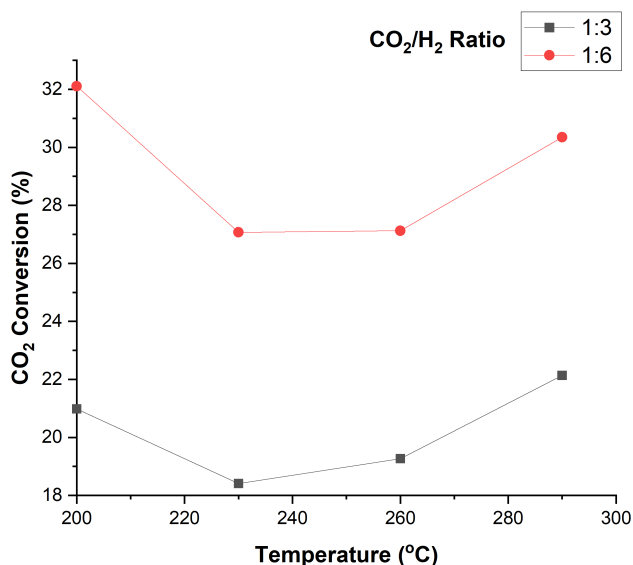


Figure 2.5: Predicted effect of Feed ratio and temperature at 20 bar on  $CO_2$  conversion for  $CO_2$  hydrogenation to methanol based on thermodynamic calculations. Methane was not considered in the equilibrium conditions.

The figure 2.5 exhibits the effect of the temperature and  $CO_2/H_2$  molar ratio on the equilibrium conversion for Carbon dioxide to methanol. It can be seen from the figure that, with the increase in the molar ratio of  $CO_2/H_2$  from 1:3 to 1:6, the  $CO_2$  conversion is increased. This suggests that

higher molar ratios can lead to increased  $CO_2$  conversion. However, increasing the molar ratio also increases the economics because it utilizes more hydrogen.

### $CO_2$ to DME

For the DME production,  $CO_2$ ,  $CO$ ,  $H_2$ ,  $H_2O$ ,  $CH_3OH$  and  $CH_3OCH_3$  components were included. Methane was not taken into account for thermodynamic calculation. The effect of the temperature and pressure for the case of  $CO_2/H_2$  ratio of 1:3 on  $CO_2$  conversion, methanol and DME selectivity are described below and shown below in the figures 2.6, 2.8, 2.7 .

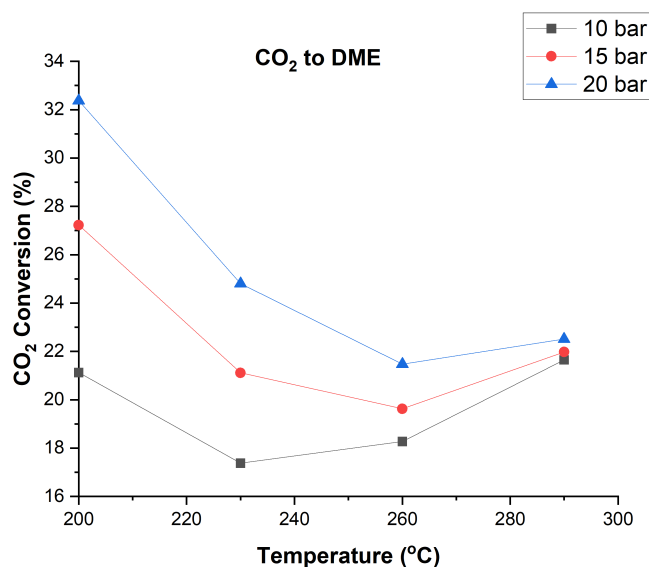


Figure 2.6: Predicted effect of temperature and pressure at  $CO_2/H_2$  ratio of 1:3 on  $CO_2$  conversion based on thermodynamic calculations. Methane was not considered in the equilibrium conditions.

The temperature ranging from 200°C to 290°C was varied with pressure from 10 to 20 bar as shown in figure 2.6 to study the effect of these parameters on  $CO_2$  conversion. Methanol synthesis and DME formation was described in the section 2.3.1. The  $CO_2$  conversion in all pressure cases, plummets with increase in temperature to a certain temperature and increases thereafter. According to Le chatlier principle, higher pressure is favorable for higher  $CO_2$  conversion, methanol and DME selectivity. The equations 2.5 and 2.7 are exothermic and favours lower temperature.

Methanol synthesis from  $CO_2$  hydrogenation is considered as the rate determining step when compared to the dehydration to DME [71]. This suggests that the thermodynamic limitation can be avoided by either increasing the pressure or removing the product and converting to DME. The conversion of Carbon dioxide is higher in the case of  $CO_2$  to DME (figure 2.6) when compared to  $CO_2$  to methanol (figure 2.3). This suggests that the thermodynamic analysis of  $CO_2$  to DME is advantageous with regards to the  $CO_2$  conversion. Moreover, it can be noted that 100% DME selectivity is hard to achieve.

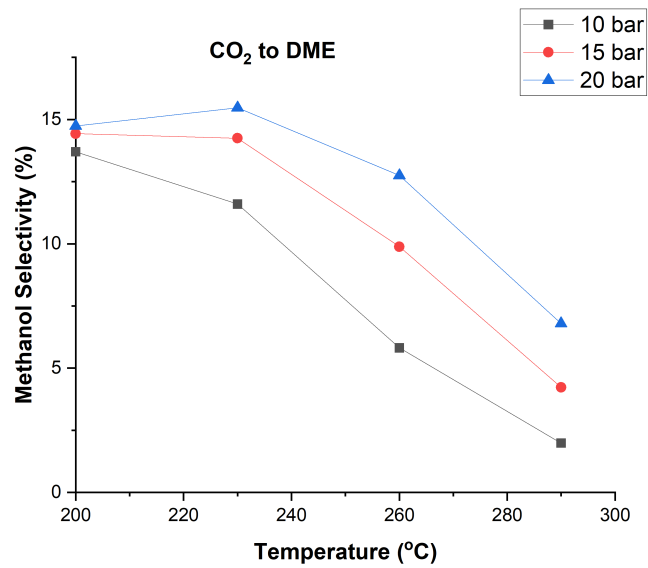


Figure 2.7: Predicted effect of temperature and pressure at  $CO_2/H_2$  ratio of 1:3 on methanol Selectivity based on thermodynamic calculations. Methane was not considered in the equilibrium conditions.

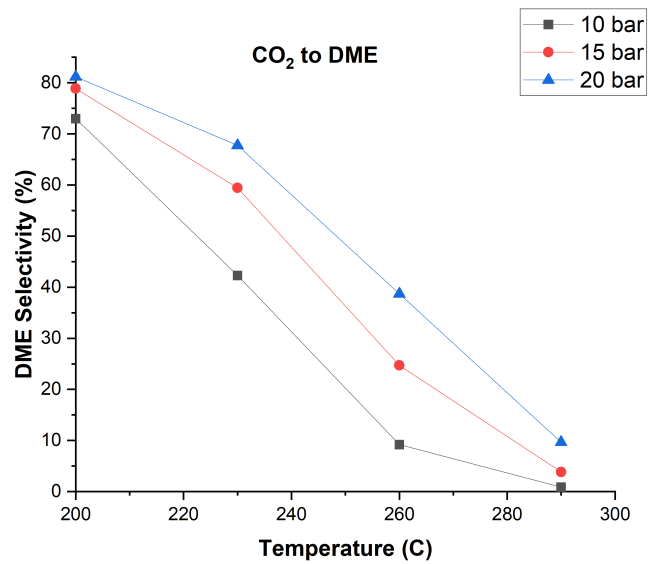


Figure 2.8: Predicted effect of temperature and pressure at  $CO_2/H_2$  ratio of 1:3 on DME selectivity based on thermodynamic calculations. Methane was not considered in the equilibrium conditions.



# Chapter 3

## Experimentation

This chapter explains the synthesis procedure of the single catalyst ( $CO_2$  to methanol) and a dual catalyst ( $CO_2$  to DME). In addition, this chapter includes the description of the reactor setup used for this research study.

### 3.1 Materials

#### 3.1.1 Single Catalysts

The single catalysts that were selected to be tested in the titanium reactor are synthesised by a Co-Precipitation method and Precipitation Impregnation method. The synthesis recipe for the  $CO_2$  to methanol i.e. single catalyst is presented below.

##### Co-Precipitation

0.2M aqueous solutions of  $Cu(NO_3)_2 \cdot 3H_2O$ ,  $Zn(NO_3)_2 \cdot 6H_2O$  and  $Na_2CO_3$  are prepared. These metal nitrate solutions and the precipitant solutions are added simultaneously drop wise into demineralised water under constant stirring of 500 rpm. A constant temperature and pH is maintained with the demineralised water. The resulting precipitate is subjected to aging at 60-65°C and constant stirring for 2 hours. The precipitate is filtered, dried and calcined at specific temperature. To obtain the CuO-ZnO/HZSM-5 catalyst similar procedure is followed, (250  $\mu m$ ) of calcined HZSM-5 is introduced into the demineralized water instead. The metal nitrate and precipitant solutions are added to it.

##### Precipitation Impregnation

0.5M and 1M of  $Zn(NO_3)_2 \cdot 6H_2O$  and Citric acid solutions are prepared. The citric acid is added dropwise into the  $Zn(NO_3)_2 \cdot 6H_2O$  solution with constant stirring. This solution is placed inside a Rotary evaporator until a viscous gel like phase is achieved. The obtained gel is further dried and the resulting powder is crushed, pelletised, sieved to the desired size and calcined.

The ZnO powder that is prepared is added to  $Cu(NO_3)_2 \cdot 3H_2O$  solution and placed in rotary evaporator. The obtained gel is subjected to drying in a vacuum oven. The resulting powder is crushed, pelletised, sieved and calcined.

##### Commercial catalysts

A commercial catalyst containing 63.5 wt% of CuO and 25 wt% of ZnO and 10 wt% of  $Al_2O_3$  and rest MgO was provided by Alfa Aesar. The commercial catalyst was crushed, sieved to the required size range (i.e. 100-250  $\mu m$ ).

### 3.1.2 Dual catalyst

The synthesis recipe for the  $CO_2$  to DME is presented below. For a methanol to DME catalyst the  $NH_4ZSM-5$  which was provided by Alfa Aesar was subjected to calcination procedure to obtain HZSM-5.

#### Co-Impregnation

0.5 M solutions of  $Cu(NO_3)_2 \cdot 3H_2O$  and  $Zn(NO_3)_2 \cdot 6H_2O$  are prepared. The solvent used in this preparation is ethanol. HZSM-5 which is a solid acid catalyst is taken and added to prepared metal nitrate solutions. The prepared solution is subjected to stirring in the rotary evaporator. The obtained blue color gel is dried, crushed, sieved into desired size and calcined.

### 3.1.3 Reagent gases and Auxiliary gas

The gases that are utilized for the experiments with the corresponding mass flow controllers are shown in the table below. In addition, a Helium (He) gas cylinder was used for leak testing. Leaks in the experimental setup were identified with a Helium leak detector. To analyse the products in the Compact-GC, Argon (Ar) and Helium (He) gases are used as carrier gas.

Table 3.1: Reagent gases and auxiliary gases used for experiments

S.no	Gas	MFC Range ( $ml_n/min$ )	MFC tag in P&ID	Reagent Purity (%)
1	Nitrogen	0-120	MFC 02	99.999
2	Hydrogen	0-500	MFC 06	99.999
3	Carbon dioxide	0-150	MFC 03	99.995
4	Compressed Air	0-150	MFC 04	-

## 3.2 Experimental setup

A semi-automated experimental setup was constructed and used to analyse and assess the process parameters on reactor performance for various catalysts. This setup was utilized to perform experiments for the production of methanol via hydrogenation of Carbon dioxide to Methanol and DME. It was capable of operating upto 20 bar of pressure. The pressure inside the reactor was maintained using a Back Pressure Regulator (BPR), that was supplied by pressure control solutions with model number LF1SNN12-NSMP5 00T300S4KKB. A Back Pressure Regulator (BPR) relieves the excess pressure when the fluid pressure is above the set point and holds back the desired pressure in the upstream. The pressure on the dome of the Back Pressure Regulator (BPR) can be released by tuning a needle valve connected to the vent.

The experimental setup 3.5 and the P&ID shown in appendix C.1 can be explained in detail in three main sections as shown in the figure 3.1. The first section is a Feeding section where components or parts related to the feed are present. The second one is a Reaction section where the reactants are reacted and converted to products. The last section is an Analytic section where the product is being analyzed. These sections are described in detail below:

### 3.2.1 Feeding section

The flow of the reactants and diluent gas to the reactor R-01 was measured and regulated using a Bronkhorst Mass Flow Controller (MFC). Each Mass flow controller is designed and calibrated to control specific gas at a particular range of flow rates. These MFCs deliver gases based on a set point that is given for the controller in LabView software. A MFC can handle a set point from 0 to 100% of its full-scale range. However, it is operated in the range from 10 to 90% where the best accuracy is obtained which is also described as the precision range for an MFC. These MFCs

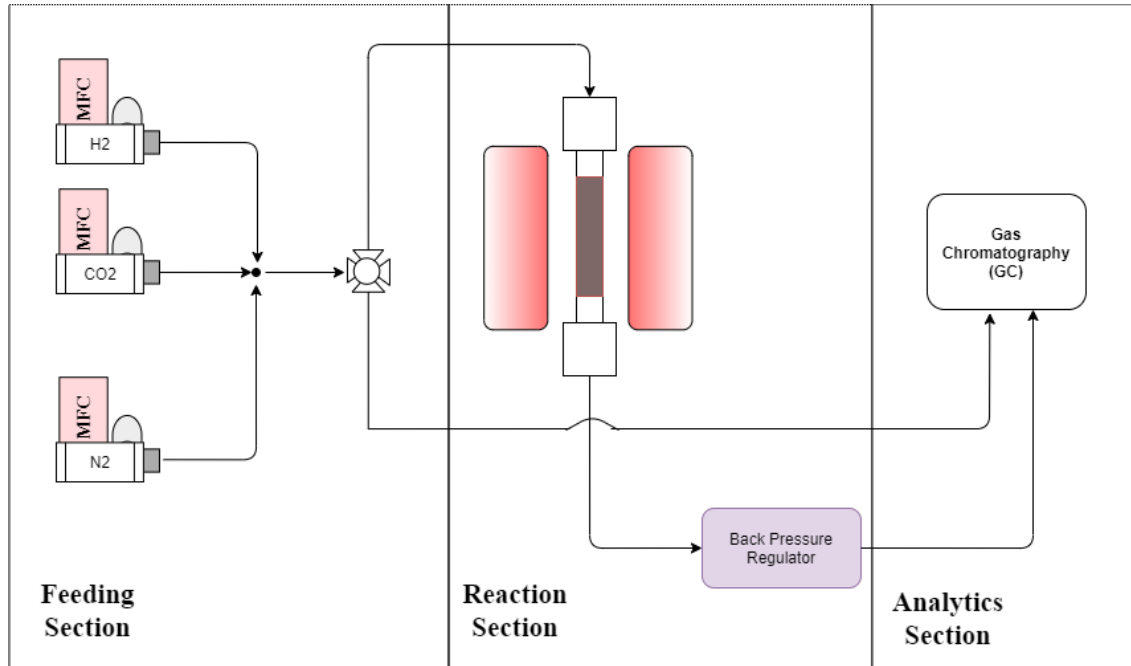


Figure 3.1: Schematic Representation of the experimental Setup

appear with a label MFC 01 - MFC 06 in the P&ID shown in the appendix C.1. Check valves are installed adjacent to the MFCs to ensure the correct gas flow directions.

The feed composition targetted for the experimentation containing Carbon-dioxide, Hydrogen, 15% Nitrogen introduced into the reactor with a desired ratio for reactions that were calculated using the Gas Hourly Space Velocity (GHSV) presented in the below equation.

$$GHSV = \frac{60 \times Q_{Total} \times (273.15 + T_{cb})}{V_{cb} \times P \times (273.15 + T_a)} \quad (3.1)$$

Where,

$Q_{Total}$  - Total flow rate of inlet gases in  $ml_n/min$

$T_{cb}$  - Temperature at the catalytic bed ( $^{\circ}C$ )

$T_a$  - Ambient temperature ( $^{\circ}C$ )

P - Pressure targetted (bar)

$V_{cb}$  - Volume of the catalytic bed

The total flow rate of inlet gases in the equation 3.1 is calculated as follows:

$$Q_{Total} = \frac{V_{CO_2} + R \times V_{CO_2}}{0.85} \quad (3.2)$$

Where,

$V_{CO_2}$  - flow of the carbon dioxide

R - ratio of  $H_2/CO_2$  (usually taken as 3)



### 3.2.2 Reaction section

This section comprises a split-tubular furnace with a titanium tubular reactor. The 2 major reasons for choosing a titanium reactor are:

1. It is capable to withstand higher pressures
2. Titanium tubular reactor was used instead of stainless steel to avoid secondary reactions on the wall of the reactor at higher temperatures (Titanium is inactive at high temperatures)

Table 3.2: Dimensions of the Fixed Bed Reactor used for experimentation

Titanium tubular reactor dimensions		
Length(mm)	Outer Diameter (OD)in mm	Inner Diameter (ID) in mm
390	9.53	7.75

A thermowell with 1mm OD was used to protect the temperature sensors or thermocouples inside the tubular reactor. This thermowell was positioned homocentric to the titanium reactor. The thermowell was coated by SilkoTek<sup>®</sup> with a silicon layer to passivate the surface. The catalyst was placed in between the thermowell and the reactor wall.

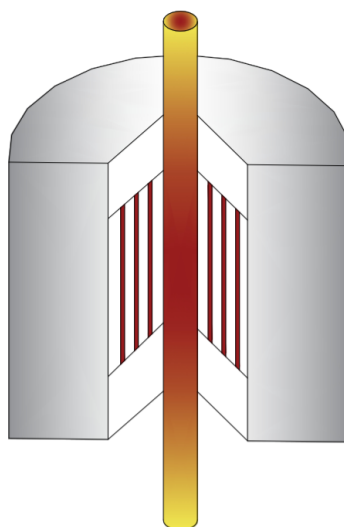


Figure 3.2: Tubular Furnace operated for providing heat to the titanium fixed bed reactor

To monitor the temperature inside the tubular reactor, two k-thermocouples were placed in the thermowell. These thermocouples were positioned at the top, middle of the reactor and tagged with TI-33, TI-34 respectively in the P&ID C.1 and PLC shown in Figure 3.3. The temperature for the titanium reactor was provided by the 3210 series split tubular furnace with a maximum temperature of 900°C and 1100 W supplied by Applied test systems as depicted in Figure 3.2.

### 3.2.3 Analytics

The products were analysed by an Interscience Compact GC (Gas Chromatograph) GC 4.0 supplied by Gas Analyser Solutions™. In general, a gas chromatograph is used for separating and analyzing the vaporised components without decomposition. The product stream after the back pressure regulator was connected to this online-GC. The products were maintained at 200°C with the aid of heat tracing and insulating bands to ensure that product stream is in gas phase. To safeguard the GC from over pressures the product stream was equipped with a safety pressure relief valve set at 2 bar. Hence, in any case if the product attains more than 2 bar pressure it is relieved. Besides, the product outlet is equipped with a water condenser that avoids water from being injected into the GC.

A sample injection of 5  $\mu\text{L}$  from the product stream was introduced into the GC. The sample that is injected is splitted into parts which results in sharp peaks in the chromatogram due to very small volume of sample. The split gas is carried by a carrier gas to the columns that were present in the respective channels as shown in the figure B.1. Helium gas was used as carrier gas for Channel-1, Channel-2, Channel-3 and Argon was used for the Channel-4. Based on the type of the column the residence time of the gases varies at the detector. The detector detects the signal and passes the information to a recorder which provides a chromatogram.

The Thermal Conductivity Detectors (TCD) that are present in the GC can detect the gases provided in the table B.2 based on the columns except the carrier gas. The temperature of the detectors is maintained at 110°C. The detector filament temperature for TCD-1, TCD-2, TCD-3 are placed at 210°C whereas, TCD-4 is maintained at 230°C. With a constant flow of carrier gas to the filaments, a base reading is established. As other gases with varying thermal conductivity approach the filament, the temperature of filament is altered. According to the Wheatstone bridge principle, the TCD varies the current to maintain a constant temperature at the filament. Hence, the change in current in a TCD is dependent on the type of gas and its concentration. The GC data visualization, accountability, equipment control are managed and operated by Chromeleon™ software.

The calibration of the detected gas components were accomplished using calibration cylinders i.e. known composition as mentioned in the appendix Table B.1. For the case of liquid component such as methanol, a 1.5L tedlar bag was used to make liquid component in known composition. The bag is filled with known amount of pure methanol liquid using a syringe and  $N_2$  gas using a MFC. The tedlar bag was provided with a on-off valve, this valve is closed after filling the Nitrogen and left untouched for sometime allowing the methanol vapor to reach equilibrium with Nitrogen gas. The tedlar bag was connected to the inlet of the GC and samples were injected.

In order to calculate the Molar flow rate in the outlet stream, equation 3.3 is used where nitrogen was fed as an inert gas which ends up in the outlet without participating in any reaction.

$$n_{TOTAL} = \frac{n_{N_2}^{in}}{x_{N_2}^{out}} \quad (3.3)$$

The above calculation aids in obtaining  $CO_2$  conversion, products selectivity and yield. The product stream contains various components, the molar flow rate (n) of these components can be calculated by multiplying the obtained Total molar flow rate from above calculation with the mole fraction of that component obtained from GC measurement. Moreover, the  $CO_2$  conversion, selectivity of each product ( $S_i$ ), and yield can be calculated using the following formulae:

$$X_{CO_2}(\%) = \frac{n_{CH_3OH}^{out} + n_{CO}^{out} + n_{CH_4}^{out}}{n_{CO_2}^{in}} \times 100 \quad (3.4)$$

$$S_i(\%) = \frac{n_i^{out}}{n_{CH_3OH}^{out} + n_{CO}^{out} + n_{CH_4}^{out}} \times 100 \quad (3.5)$$

$$Y_i(\%) = \frac{Conversion \times Selectivity}{100} \quad (3.6)$$

For the case of  $CO_2$  to DME the  $CO_2$  conversion, Selectivity of DME and yield is calculated by :

$$X_{CO_2}(\%) = \frac{n_{CH_3OH}^{out} + n_{CO}^{out} + n_{CH_4}^{out} + 2 \times n_{DME}^{out}}{n_{CO_2}^{in}} \times 100 \quad (3.7)$$

$$S(\%) = \frac{2 \times n_{DME}^{out}}{n_{CH_3OH}^{out} + n_{CO}^{out} + n_{CH_4}^{out} + 2 \times n_{DME}^{out}} \times 100 \quad (3.8)$$

$$Y_i(\%) = \frac{Conversion \times Selectivity}{100} \quad (3.9)$$

Considering the variance between the repeated experiments and the precision of the equipment, the reported values of selectivity, conversion, and yield has an average of  $\pm 10\%$  error margin around their shown actual values. This indicates that for instance, the actual value of methanol yield lies in the range of  $0.9 \times DME - Yield^{reported} < DME - Yield^{actual} < 1.1 \times DME - Yield^{reported}$

### 3.2.4 Reactor automation

To observe the process variables such as temperatures, pressures, flow rates and other vital parameters, LabVIEW was used. Besides, these process variables are controlled via a Programmable Logic Controllers (PLC) that was designed in LabVIEW programme as shown in the figure 3.3. The desired set points for these process variables are inputted and the measured values are monitored throughout the experimentation. This programme enables the reactions and the process variables in control configured limits. The inlet and outlet pressure of the reactor was monitored constantly. The flow of  $CO_2$ ,  $N_2$ ,  $H_2$  shown in the below PLC figure 3.3 are the input given for  $CO_2/H_2$  1:3 ratio at  $200 h^{-1}$  GHSV,  $200^\circ C$  and 15 bar. It is to be noted that the 3rd thermocouple which is shown as TI-35 in the figure 3.3 is not in use/working condition.

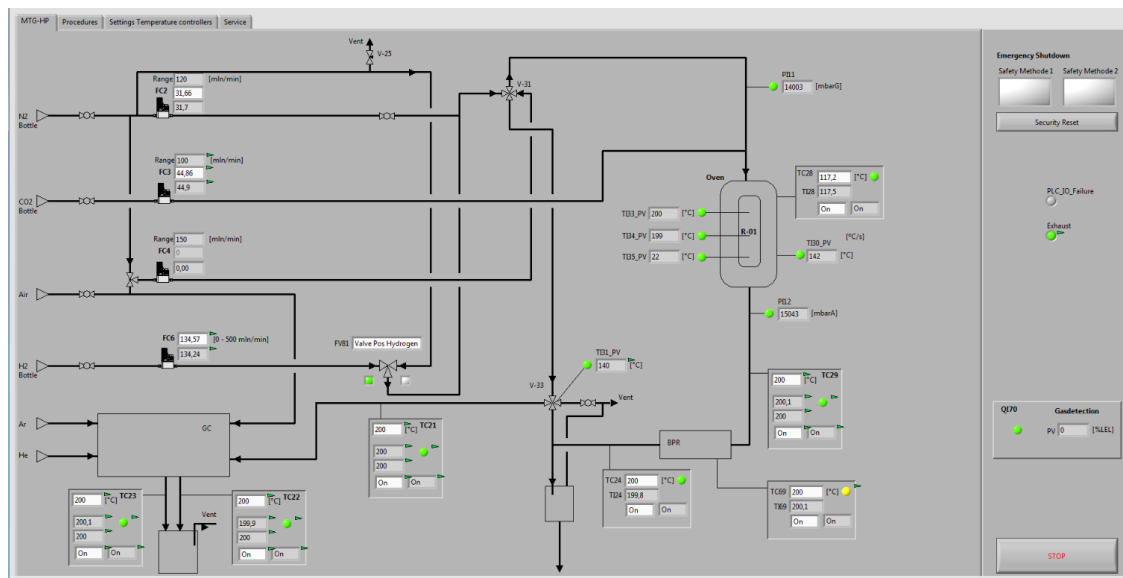


Figure 3.3: Programmable Logic Controller (PLC) of the experimental setup

### 3.3 Methods

A standard operating procedure was developed and followed during assembling the catalyst in the reactor and pressurizing the reactor system. The loading of catalyst into the titanium reactor is described below. A proper care has to be accounted while filling the catalyst inside the reactor. In case of improper loading of the catalyst in the reactor, it could lead to channeling of gases or higher pressure drop across the catalyst bed.

#### 3.3.1 Catalyst Assembling

The assembling of the catalyst plays a vital role in the experimentation. The selected catalysts that were presented in section 3.1.1 and 3.1.2 were tested in the fixed bed reactor. The size range for catalysts targetted for testing in the titanium reactor was 100-250  $\mu\text{m}$ . The catalyst is placed in the middle of the split tubular heating furnace section. In order to position the catalyst in the middle of the reactor. Firstly, the reactor was closed on the bottom with a quartz wool as clearly shown in the figure 3.4. Secondly, inert beads were utilized to fill the reactor till the desired height and covered with quartz wool. Finally, the sieved catalyst was placed inside and secured with quartz wool on the top.

The reactor is tapped gently while filling the catalyst to ensure the catalyst settles on the quartz wool bed uniformly. Filters were installed on the top and bottom of the reactor. The top filter ensures no foreign particles enters the reactor zone whereas the bottom one protects from any particles leaving the reactor. For the case of a two layered catalyst, the methanol to DME catalyst is placed on the quartz wool first and  $\text{CO}_2$  to methanol catalyst is placed on top of it. The same order or pattern follows for the 10 layered catalyst. In order to determine the amount of catalyst required for the reaction, inner diameter of the titanium reactor, density of the catalyst were taken into account for calculation.

The reactor was installed into the setup after filling the required amount of catalyst for the reaction. A leak test was performed by pressurizing the reactor at constant temperature, while inlet and outlet streams are closed. The leaks in the experimental setup can be noticed by monitoring the system pressure. In case a leak is observed, it is identified either by applying a leak

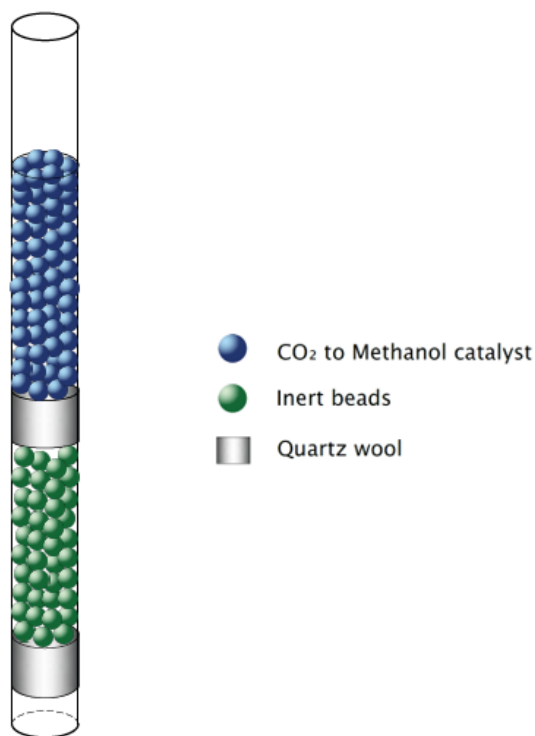


Figure 3.4: Methanol synthesis (single) catalyst arrangement inside the Titanium Reactor

detector solution on the valves and seals or by using an electronic leak detector provided by Restek. Thereafter, the catalyst needs to be reduced prior to each test or reaction.

### 3.3.2 Catalyst Reduction

In order to activate the catalyst before performing a reaction, the catalyst was exposed to a reduction phase where 100  $ml_n/min$  of hydrogen gas was passed through the reactor bed for a duration of 1 hour at a temperature of 300°C and ambient pressure. To achieve the required temperature for reduction, nitrogen gas was used with proper flow rate while the desired temperature is set in the LabView software.

### 3.3.3 Reaction

Subsequent to the catalyst reduction the reactor was cooled down to the required reaction temperature by using proper amount of Nitrogen gas. The pressure was set in the system using a pressure reducer that enables pressures on the BPR to match the desired reaction pressure. The temperatures of all lines were maintained at 200°C by using heat tracing. This heat tracing avoids condensation of products in the lines. The moment the desired reaction temperature was achieved on the catalytic bed, the feed gases were introduced into the system based on the GHSV calculation as mentioned in equation 3.1. Increasing or decreasing the pressure for the reactions is done by fine tuning the pressure reducer PI-13 shown in the P&ID shown in appendix C.1. A stabilization time of 25 to 30 mins was accounted and the samples were injected into GC.

### 3.4 Safety Aspects of the Experimental Setup

In general, a gas sensor will always indicate if the atmosphere is far away from building an explosive gas mixture in the experimental set-up. To identify this, one gas sensor is placed inside the experimental setup fume hood which can be seen in the below figure. Another gas sensor is placed outside the experimental setup. Hydrogen in terms of quantity and the nature, is the only component in this system which needs to be continually measured and have a sensor to take an action if its leaked concentration reaches the alarm levels. To detect the leaks, Hi alarm is placed at 10% of Lower Explosive Limits (LEL) and HiHi alarm is placed at 20% LEL with the sensors.

Table 3.3: Lower and Upper Explosive Limits of Gases

Gas	Limit in Air, Vol%	
	Lower	Upper
$H_2$	4	75
Methanol	6.7	36

To guarantee the safe operation of the set-up and to avoid any explosion hazard, the Item rack/fume hood is provided with two sensors for monitoring the ventilation. In case one or the two sensors detect that the ventilation stopped working, then the set-up will automatically shut down. In case of any emergencies, two safety methods are activated based on the event. In case the pressure in the system is above 20 bar, the LabView activates a safety method where all the MFCs are closed and the tubular oven is switched off. If a gas alarm triggers or the temperature inside the setup is greater than  $320^{\circ}\text{C}$  another safety method is activated to minimize the risks, by closing the all MFCs except Nitrogen MFC (used for cooling). In addition, the tracing lines and the tubular oven is turned off. A flame arrestor provided by WITT was installed in the setup with the compressed air line adjacent to the air MFC and can be seen with FA-01 tag in the P&ID C.1. This flame arrestor protects against dangerous reverse gas flows.

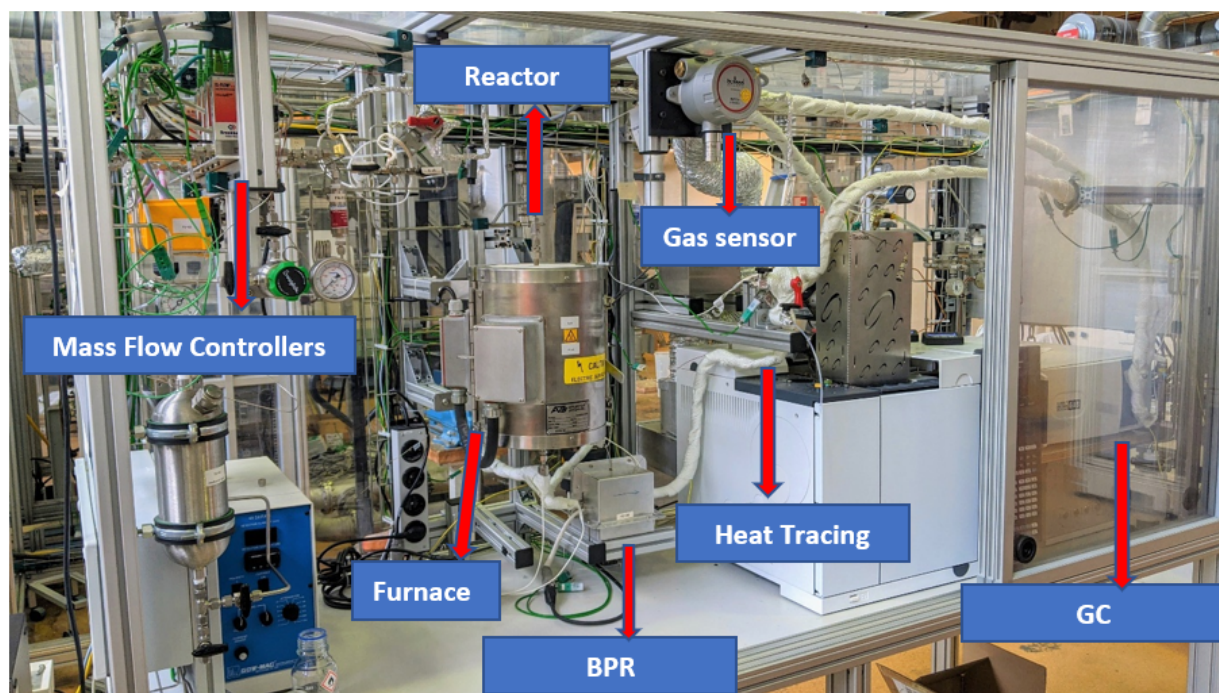


Figure 3.5: Experimental Setup in the laboratory used for testing



# Chapter 4

## Results and Discussion

### 4.1 Catalytic performance of $CO_2$ Hydrogenation Catalyst

The results in this section is described in the sequence below:

1. Comparative Performance analysis of single catalysts and screening the catalysts
2. Layering of  $CO_2$  to methanol synthesis catalyst with methanol to DME synthesis catalyst
3. Performance of a Dual catalyst
4. Sensitive Analysis of Dual Catalyst

#### 4.1.1 Comparative Performance and Screening of the Catalysts

Primarily, the Cu-ZnO catalysts that were prepared via Co-Precipitation (CP) and Precipitation Impregnation (PI) methods that were described in the 3.1.1 were tested at various temperatures ranging from 200°C to 260°C at 20 bar pressure. These Cu-ZnO based catalysts are evaluated and compared with commercial benchmark Low Pressure Methanol Catalyst (LPCC) containing Cu/ZnO/ $Al_2O_3$ . The experiments were repeated and the standard deviation was observed to be less than 5%. This indicates that the experiments were repeatable. CO and methanol were identified as the main products in the case of Carbon dioxide hydrogenation to methanol and a trace quantity of methane was measured in the GC.

The experimental data of the single catalysts ( $CO_2$  to methanol) is plotted below. Similar trends were observed with the  $CO_2$  conversion, Methanol selectivity and yield in the case of the Co-Precipitation catalyst containing Cu-ZnO and LPCC catalyst containing  $Cu-ZnO-Al_2O_3$ . It can be seen from the figure 4.1 that the  $CO_2$  conversion increases with increase in the temperature from 200°C to 260°C. The Co-Precipitation catalyst has higher conversion of carbon-dioxide compared to the synthesised Precipitation Impregnation catalyst. The conversions of the single catalysts at 200°C and 230°C temperatures are lower than the thermodynamic conversion. At 260°C the  $CO_2$  conversion of the LPCC catalyst and Co-Precipitation catalyst reached thermodynamic equilibrium conversion. Besides, the figure 4.2 represents the selectivity of the methanol for the catalysts. The plot shows a decreased trend with elevation of temperatures from 200°C to 260°C. This suggests that the methanol selectivity is favoured at lower temperatures. PI catalyst has higher selectivity to methanol but lacks conversion of  $CO_2$  which results in a lower yield of methanol.

In addition, it can be noted from the plot 4.4, the CO selectivity is increased with increase in temperature. This is due to the endothermic nature of the RWGS reaction. It can be observed from the 4.3 that the Low Pressure methanol Commercial catalyst demonstrated the highest yield at 230°C (7%) when compared to the synthesised Co-Precipitation (Co-Preci) Catalyst (4.7%)



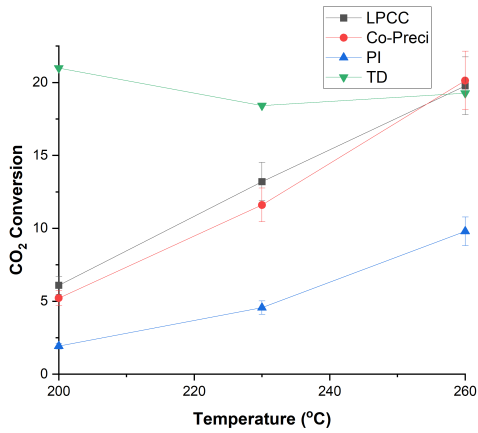


Figure 4.1: Effect of temperature on  $CO_2$  Conversion for single catalysts at 20 bar pressure and  $400 h^{-1}$

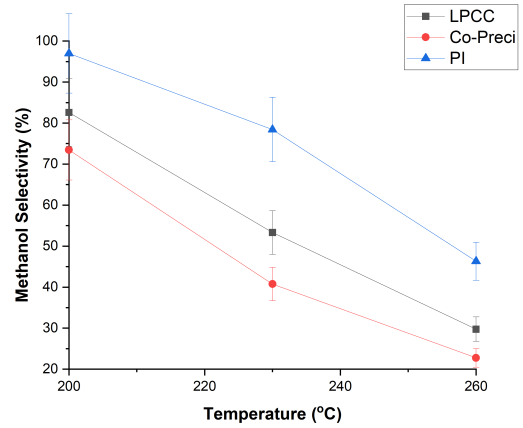


Figure 4.2: Effect of temperature on methanol selectivity for single methanol synthesis catalysts at 20 bar pressure and  $400 h^{-1}$

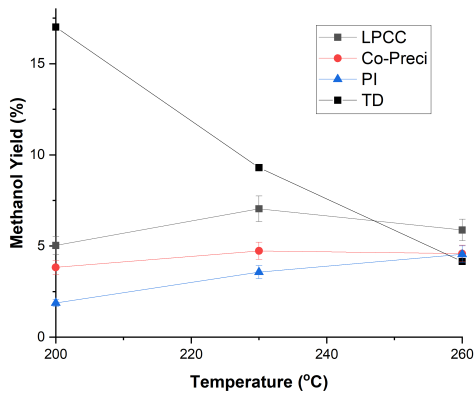


Figure 4.3: Effect of temperature on methanol yield for single catalysts at 20 bar pressure and  $400 h^{-1}$

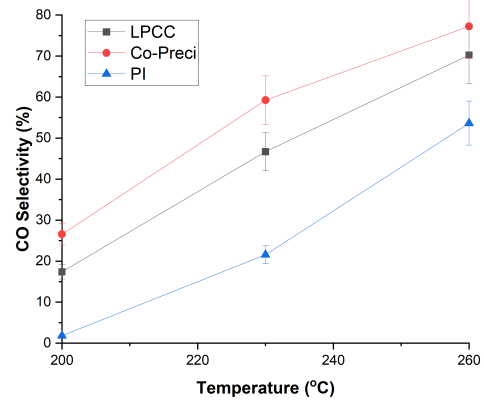


Figure 4.4: Effect of temperature on CO selectivity for single catalysts at 20 bar pressure and  $400 h^{-1}$

and Precipitation Impregnation (PI) catalyst (3.57%) at same temperature. This is due to its better catalytic activity of the Commercial catalyst. Looking at the performance of the synthesised catalysts, Co-Precipitation catalyst has greater yield at all tested temperatures compared to the Precipitation Impregnation catalyst. This is due to the low copper content present in the PI catalyst which can be seen in the table A.2.

### Effect of Feed ratio

The Co-Precipitation catalyst is taken for further analysis to observe the behaviour of conversions, methanol selectivity at higher feed ratios. As per the equation 2.5, the reaction stoichiometry demands a  $CO_2/H_2$  of 1:3. Figure 4.5 (a) illustrates that the increase in  $CO_2/H_2$  ratio from 1:3 to 1:6 has shown a significant increase in the conversion of  $CO_2$  at all tested temperatures ranging from 200°C to 260°C. The conversion of carbon dioxide for both the ratios stayed lower than or equal to the thermodynamic equilibrium conversion.

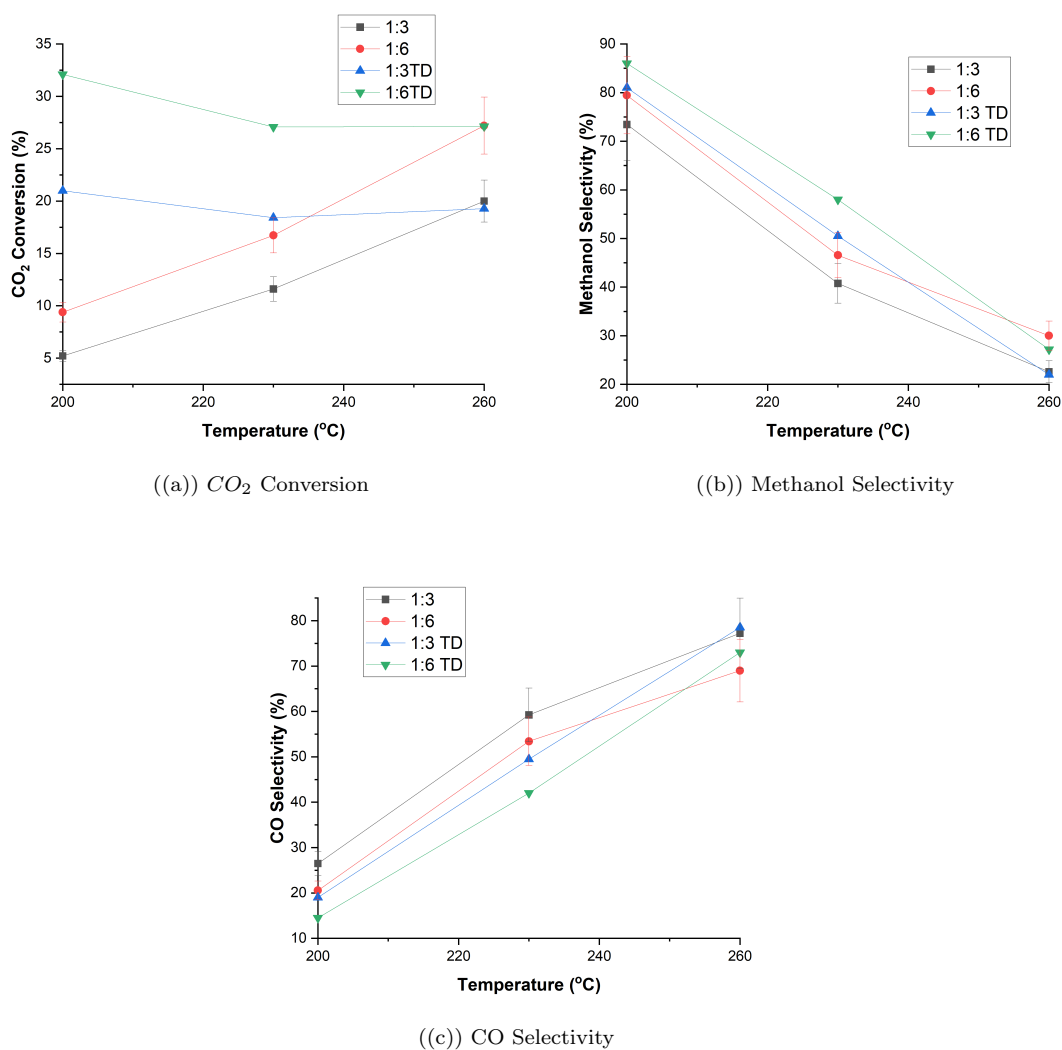


Figure 4.5: Effect of Feed ratio on  $CO_2$  conversion, methanol and CO selectivity for Co-Precipitation Catalyst. Reaction conditions: Pressure= 20 bar, GHSV =  $400 h^{-1}$

In the figure 4.5 (b), Methanol selectivity is plotted for 1:3 ratio and 1:6 ratio. The methanol selectivity decreases with increase in temperature from 200°C to 260°C in both the tested ratios. The selectivity of the methanol has increased at all tested temperatures while the  $CO_2/H_2$  ratio has increased from the 1:3 to 1:6. Besides, the thermodynamic equilibrium selectivity of methanol for these ratios is also plotted. At the temperatures, 200°C and 230°C the selectivity of methanol is below the thermodynamic equilibrium selectivity. However, at 260°C temperature, the selectivity of methanol has reached the thermodynamic equilibrium which is still observed in the error range. The fig 4.5 c describes the behaviour of CO selectivity at both ratios (i.e. 1:3 and 1:6). It can be seen that the selectivity of CO increases with elevation of temperatures. Similar to the Conversion of  $CO_2$  and methanol selectivity the CO selectivity has also increased with rise in the ratio. It can be noticed that the CO selectivity is higher than the thermodynamic equilibrium values. The same trend with CO selectivity was observed by Arena et al. [72].

An improvement was observed with  $CO_2$  conversion and selectivity of methanol at higher ratio (1:6) when compared to 1:3. Moreover, using higher ratio of hydrogen to carbon dioxide in the feed shifts the equilibrium towards product side [62]. However, the experimentation in the next section is concentrated in lower ratio of  $CO_2/H_2$  i.e. 1:3 to save the hydrogen as it is very expensive and affects the economics.

### 4.1.2 Spatially arranged catalytic bed $CO_2$ to DME

A detailed study was performed with physically mixed or spatially arranged i.e. 2 layers, 10 layers of catalyst. The titanium fixed bed reactor was filled with Co-Precipitation catalyst which demonstrated a better performance for methanol synthesis in the previous section 4.1.1 was combined with solid acid catalyst which is responsible for methanol to DME as shown in the figure 4.6. The first configuration in the 4.6 is a dual bed or a 2 layer configuration where the methanol to DME catalyst is placed in the reactor at the bottom and the  $CO_2$  to methanol catalyst is placed on the top. The second bed configuration is a multi layered concept where the methanol synthesis catalyst and the methanol to DME synthesis catalyst are placed consequently. The third bed configuration is a mixture of both the catalysts loaded into the reactor. The main reasons for choosing these type of configurations are mentioned below:

1. Single reactor usage instead of two
2. Bridging the active sites between methanol synthesis catalyst and methanol dehydration catalyst in macro scale.
3. Methanol converted from methanol synthesis catalyst will be converted to DME in presence of solid acid catalyst.
4. Overcoming the thermodynamic equilibrium constraints in methanol synthesis

It should be noted that the density of methanol dehydration catalyst is 50% lower when compared to the methanol synthesis catalyst. Hence, the ideal catalytic bed was made of equal volume of these catalysts. Therefore, the weight percentage of the methanol synthesis catalyst to DME synthesis catalyst was placed in 2:1 ratio which was kept constant in these bed configurations to evaluate the effect of catalyst arrangements in the fixed bed reactor. The bed configurations were focused to be tested at a lower GHSV for better yield of methanol as mentioned in the literature [49] [73]. The methanol that is produced from the methanol synthesis catalyst converts to DME in presence of solid acid catalyst. In order to this, the bed configurations are tested at 200  $h^{-1}$  GHSV which is the lowest possible GHSV achievable in the experimental setup based on the GHSV equation 3.1 and flow limitations present with the Mass Flow Controllers.

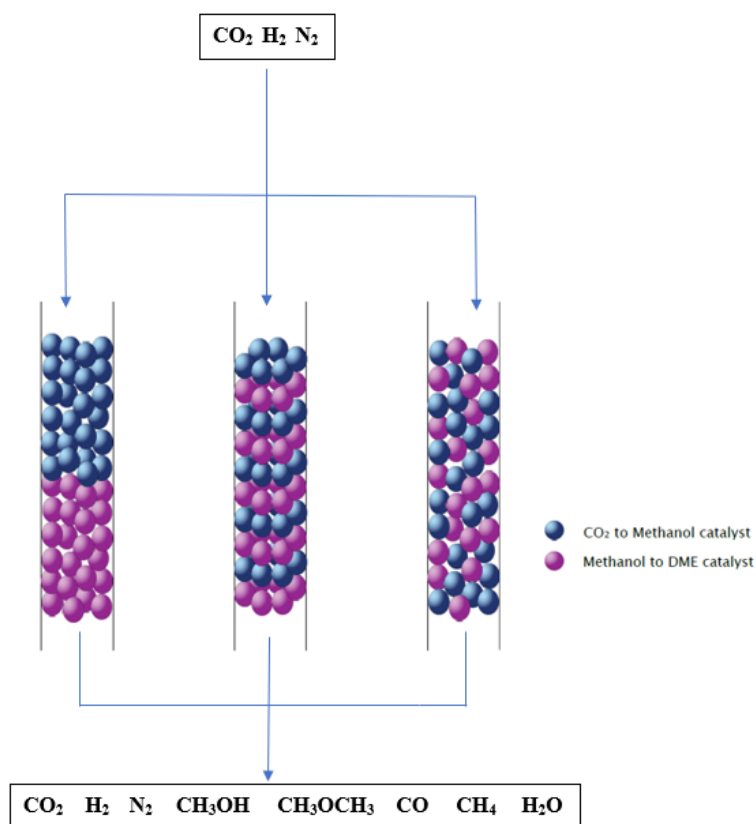


Figure 4.6: Different methods for combination of methanol synthesis catalyst with methanol to DME catalyst : Left) achieved by loading a layer of DME synthesis catalyst (pink) and a layer of methanol synthesis catalyst (blue) , Middle) achieved by loading multiple layers of methanol synthesis catalyst and Solid acid catalyst (10 layers), Right) Physical mixture of  $CO_2$  to methanol catalyst with solid acid catalyst

The selectivity of methanol and DME together for the case of 2 layer, 10 layer, and physical mixing with varied temperature ranging from  $200^\circ C$  to  $260^\circ C$  at 10 to 20 bar pressure can be seen in the surf plot shown in fig 4.7. It can be observed from the surf plot that the steadily converting the methanol that is produced to DME in a step by step manner has improved the combined selectivity of the methanol and DME. The same phenomenon applies in the case of physical mixture of both catalysts. The combined methanol and DME selectivity for the 10 layer bed configuration is highest at 20 bar and  $200^\circ C$  (i.e. 98% ) compared to the physical mixing and 2 layer bed configurations which is 96% and 89% respectively. In addition, figure 4.7 illustrates that the selective conversion of carbon dioxide to the desired products i.e (Methanol and DME) can be enhanced using the proper arrangements of the catalysts. This improvement can be noticed clearly in some operating conditions.

The influence of pressure in the bed configurations can also be seen in the surf plot 4.7 with varied temperature. Increase in the pressure has increased combined selectivity of the DME and methanol very slightly. This could be due to the adsorption of water on the catalyst surface with elevation of pressure [69]. Therefore, the optimised pressure was chosen as 15bar.

The figure below 4.8 shows yields of the desired products at 15 bar pressure,  $200\ h^{-1}$  GHSV,

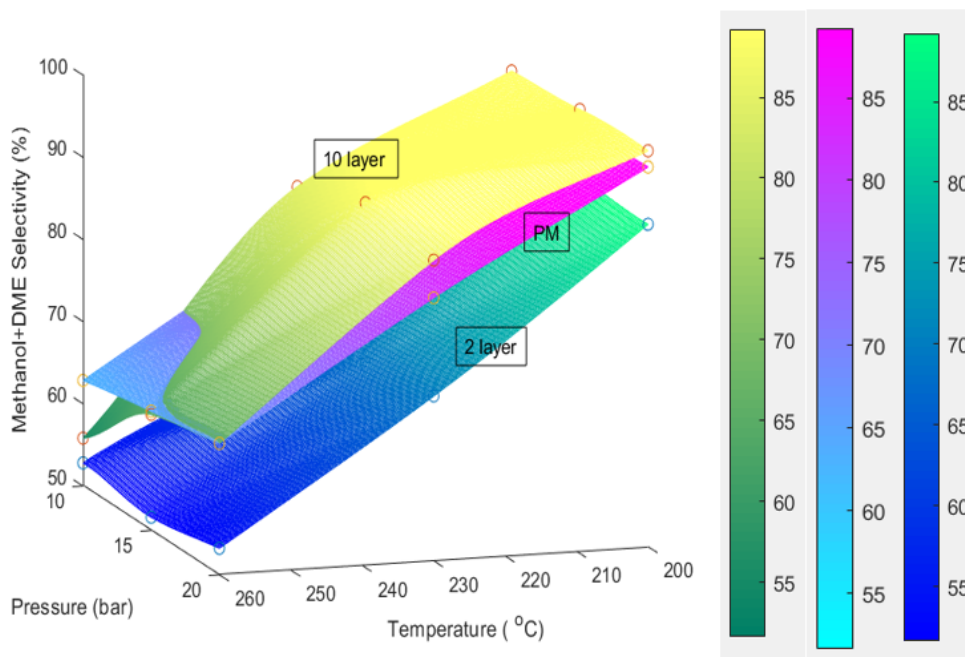


Figure 4.7: Combined methanol and DME selectivity for the tested bed configurations. Reaction conditions:  $CO_2/H_2$  ratio =1:3, GHSV=  $200 h^{-1}$ . unfilled circles (o) represents the tested reactor results

$CO_2/H_2 = 1:3$  ratio for the bed configurations. The combined yield of methanol and DME was highest at all tested temperatures in the case of physical mixing which can also be termed as infinite layers compared to 2 layer and 10 layer. The same phenomenon was also observed in the simulation of McBride et al. for the direct synthesis of DME from syngas. [56]. The highest yield (i.e. 15.7%) was observed at  $230^\circ C$  in physical mixing method while 10 layer and 2 layer resulted 15% and 14% respectively. This could be explained due to the presence of the methanol synthesis catalyst active sites very close to the DME synthesis catalyst active sites in a physically mixed catalytic bed configuration. At the optimum temperature  $230^\circ C$ , the combined yield of methanol and DME reduced from 15.7% to 14% when the number of layers decreased from infinite (i.e. Physically mixed) to 2.

In addition, Co-Precipitation single catalyst was also tested at the same GHSV, temperature, and pressure as a reference. It is worth noting that the selectivity of methanol and  $CO_2$  conversion for Co-Precipitation single ( $CO_2$  to methanol) catalyst tested at  $200 h^{-1}$ , 15 bar and  $230^\circ C$  is 34% and 15% respectively while physical mixing resulted better conversion (i.e. 19.4%) and combined methanol and DME selectivity of 81%. This indicates that the methanol synthesis thermodynamic equilibrium constraints in methanol synthesis have been mitigated using the additional catalyst to produce DME.

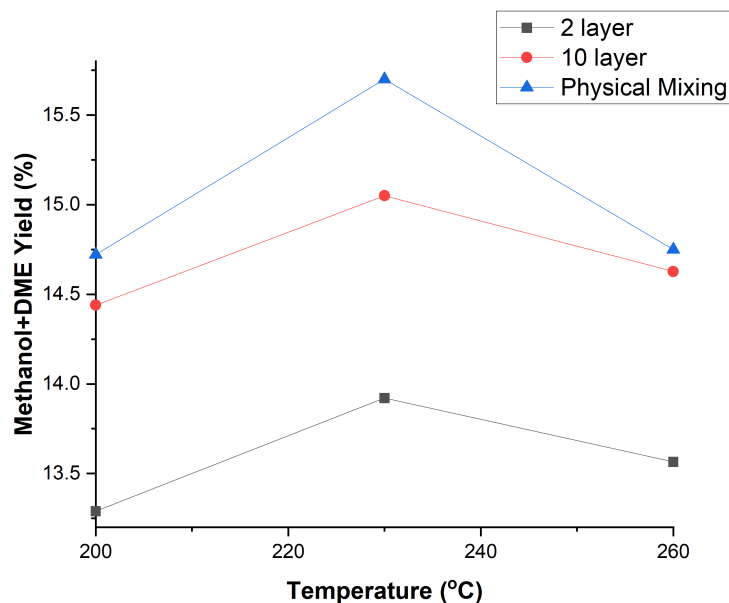


Figure 4.8: Combined yield of methanol and DME for bed configurations containing methanol synthesis and methanol to DME catalysts.

Reaction conditions: Pressure= 15 bar GHSV=  $200\text{ h}^{-1}$  and  $\text{CO}_2/\text{H}_2$  ratio = 1:3

### 4.1.3 Performance of Dual Catalyst

The Co-Impregnation dual catalyst that is described in 3.1.2 was tested at  $200\text{ h}^{-1}$ , 15 bar, 1:3 ratio of  $\text{CO}_2/\text{H}_2$  for varied temperature. This catalyst contains a composition of 2:1 wt(%) which translates to higher HZM-5 content compared to methanol synthesis catalyst. The performance of this catalyst at various operating conditions are reported below.

#### Effect of Temperature

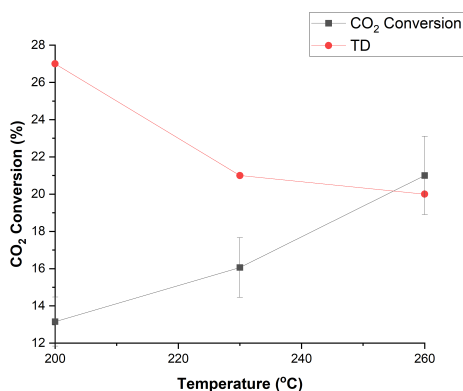


Figure 4.9: Effect of temperature on  $\text{CO}_2$  Conversion for a Co-Impregnation dual catalyst

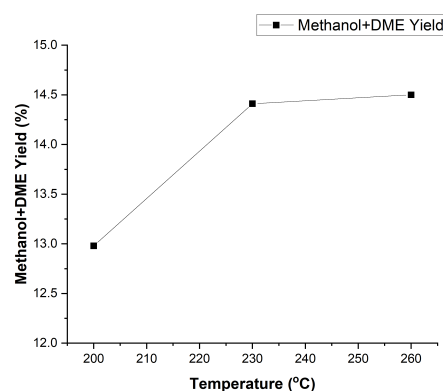


Figure 4.10: Effect of temperature on Summation of methanol and DME yield

The figure 4.9 shows the conversion of the carbon dioxide for  $\text{CO}_2$  hydrogenation to DME over the CuO-ZnO/HZSM-5 Co-Impregnated dual catalyst under 15 bar pressure with varied

temperature ranging from 200°C to 260°C. The figure illustrates that the conversion of  $CO_2$  increases with elevation of temperatures. It can be observed that the conversion has increased from 13% to 21% when the temperature rose from 200°C to 260°C. In the figure 4.10 an increase in the yield of methanol and DME together increased when the temperature rose from 200°C to 260°C. The highest yield of the methanol and DME is observed at 260°C which is 14.5% when compared to 13% at 200°C. As per Arrhenius equation, increasing the temperature improves the reaction rate constant which results in enhancing the reaction rate for the DME synthesis. Nevertheless, increasing the temperature above 260°C has a negative impact on the DME yield [74]. Hence, the further analysis is performed at 260°C.

### Effect of GHSV

The CuO-ZnO/HZSM-5 catalyst synthesised for the  $CO_2$  to DME is further investigated to study the influence of GHSV at 260°C, 15 bar pressure and  $CO_2/H_2$  ratio of 1:3. In the figure 4.11, it can be noticed that the conversion of  $CO_2$  has decreased from 21.8% to 19.7% and the combined yield of methanol and DME decreased from 14.47% to 13.7% while the GHSV is increased from 200  $h^{-1}$  to 400  $h^{-1}$  respectively. This is attributed to the contact time between the mixture of the feed gases i.e  $CO_2$  and  $H_2$  and the catalyst surface decreasing with increase in the GHSV[73] [49].

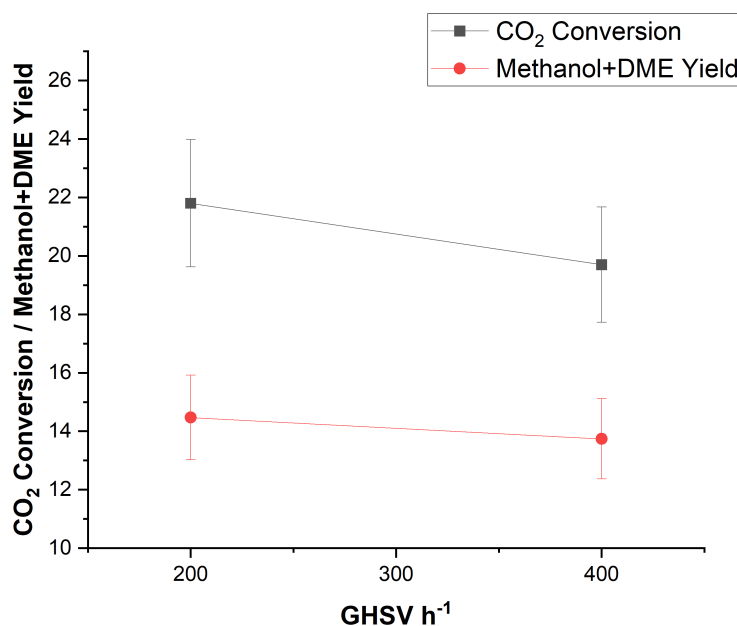


Figure 4.11:  $CO_2$  conversion and combined methanol and DME yield for a Co-impregnated dual catalyst

Reaction Conditions: Pressure = 15 bar , Temperature = 260°C,  $CO_2/H_2$  ratio =1:3

#### 4.1.4 Sensitivity Analysis

The sensitivity analysis of the parameters was investigated using the Yates algorithm which utilizes two level full factorial design. The experiments were designed in a specific arrangement (i.e. Yates order) to identify the predominant parameter influencing the performance. The table below shows the design of the experiments conducted for this study using 3 parameters namely temperature, GHSV,  $H_2/CO_2$  ratios at two levels being the lower level and higher level. These set of operating parameters shown in table 4.1 were tested with a repetition to calculate the most significant parameter influencing the Methanol+ DME yield.

S no	Temp °C	GHSV	$H_2/CO_2$ ratio	TC	Methanol + DME yield	Column-3*	Equivalence
1	200	200	3	1	12.27	101.17	Total
2	260	200	3	a	14.28	8.07	4 eff (a)
3	200	400	3	b	10.96	-4.82	4 eff (b)
4	260	400	3	ab	13.35	-2.2	4 eff (a×b)
5	200	200	6	c	11.64	-0.60	4 eff (c)
6	260	200	6	ac	14.78	-0.72	4 eff (a×c)
7	200	400	6	bc	11.65	-0.35	4 eff (b×c)
8	260	400	6	abc	12.19	-2.97	4 eff (a)

Table 4.1: Results reported using Yates analysis showing the design of experiments used to identify the most significant parameter tested at constant pressure of 20bar

\* Detailed calculation is shown in the appendix D.1

Table 4.1 contains the combined methanol and DME yield obtained for the conducted tests using Co-Impregnation dual catalyst at 20 bar. The treatment combinations denoted with TC in the table represents the level of variation of parameters. Based on the procedure and the detailed calculation presented in the appendix D.1, the values reported under column-3 have been calculated. These values indicate the relative importance of effect of each parameter and their possible interactions. The positive values appear in the column-3 corresponds to a positive effect of increasing that specific parameter or interaction of parameters on improving the combined methanol and DME yield. The negative values indicates the negative effect of corresponding parameter or the interactions of parameters. Treatment Combination 1 shows the summation of the effects of all parameters and their interactions. Treatment Combination-a resulted the highest value in the column-3 indicating a significant impact of increasing the temperature (up to 260°C) on improving the combined methanol and DME yield. Varying temperature has the most significant impact on the combined methanol and DME yield that has been reflected through the previously reported trends (e.g. Figure 4.10) in this thesis. We have observed such a sensitive behavior toward reaction temperature all through the experimentation and therefore always tried to control the reaction temperature as precise as possible. Treatment combination-b is the next highest absolute value after treatment combination-a with a negative value. This indicates that in the considered range of variation of these parameters, increasing the GHSV from 200  $h^{-1}$  to 400  $h^{-1}$  significantly decrease the combined methanol and DME yield. This has been also previously reported to be an important parameters as for instance shown in Figure 4.11. Similarly, the effects of other parameters could be analyzed.





## Chapter 5

# Conclusions

Converting  $CO_2$  into added value products such as methanol and DME significantly contribute in reducing the rate of global warming and advancing the field of sustainable fuel and chemicals production.

An experimental setup was retrofitted to test catalytic hydrogenation of carbon-dioxide to methanol and DME while securing a safe and robust operation. The process parameters such as the temperature, pressure and feed flows were monitored and controlled via LabView control system. This setup enabled investigating the effects of temperature, pressure and GHSV on the reactor performance. A comprehensive performance analysis on various catalysts and catalytic bed arrangements of  $CO_2$  hydrogenation and methanol-dehydration catalysts was performed with regard to the variation of these parameters. This includes analyzing the results of the reactor tests of  $CO_2$  hydrogenation to methanol single catalyst, sequence of layers of  $CO_2$  hydrogenation and methanol-dehydration catalysts, mixture of these catalysts and dual-catalysts for direct DME production. The results indicated the importance of homogeneous distribution of the active sites and the undesired effect of water on the selective performance of this catalytic system.

The methanol yield obtained from the synthesized single catalysts were compared with the recorded yield of commercially available reference catalyst. The commercial catalyst at  $230^\circ C$  showed a highest methanol yield (7%) compared to the methanol yield recorded for Co-Precipitation catalyst (4.7%) and for the Precipitation Impregnation synthesized catalyst (3.57%). The highest yield obtained by the commercial methanol catalyst is due to its relatively high catalytic activity as it contains higher CuO. The catalyst synthesized by precipitation impregnation showed the lowest yield of methanol at this stage partially because of its relatively low CuO content.

The direct  $CO_2$  hydrogenation to DME has been studied using various bed configurations by spatially arranging/ physically mixing the catalysts. The best performed Co-Precipitation catalyst among the synthesised catalysts was assembled in a bed with a commercial HZSM-5 catalyst which is responsible for methanol dehydration. Converting the produced methanol to DME in a step by step manner (i.e 10 layer and physical mixing) has resulted in higher selectivity towards the desired products. The summation of methanol and DME yield was enhanced while the distance between the two catalysts reduces. The closest distance was achieved in case of physical mixing assuming an infinite number of catalytic layers. Besides, the single Co-Precipitation catalyst exhibited a methanol selectivity of 34% and  $CO_2$  conversion of 15%. The combination of the same catalyst with HZSM-5 in a physical mixing bed resulted a conversion of 19.4% and combined methanol and DME selectivity of 81%.

To investigate how significant the impacts of the parameters and the operating conditions on the performance of the dual catalyst are, a sensitivity analysis was conducted using Yates algorithm. The results indicate that the reaction temperature was the most significant parameter

influencing the combined yield of desired products. Beside the significant positive effect of temperature (clearly recorded at 260°C), lowering the GHSV to 200  $h^{-1}$  usually also enhances the combined yield of desired products.

It was demonstrated that methanol production, which ultimately appear, can be significantly improved and in fact could reach beyond thermodynamically estimated value of methanol production under some sets of operating conditions when methanol is efficiently converted to DME.

The results and conclusions presented in this research can be used further for tailoring the dual catalytic structure.

## Chapter 6

# Outlook

Ensuring a fast conversion of methanol to DME and removal of water significantly improve the  $CO_2$  conversion and selective DME production by shifting the reactions equilibrium. The hindering effect of water on the performance of the methanol synthesis catalyst and methanol dehydration catalyst can be investigated by feeding water in the reactor inlet along with the feed reactants. Moreover, the water that is produced during the methanol synthesis reaction and the Reverse Water Gas shift reaction could be selectively removed insitu using adsorption techniques or a membrane. This solves the problem by avoiding the catalyst deactivation due to water adsorption. In addition, the equilibrium shifts towards the desired products, namely methanol and DME.



# Acknowledgement

Firstly, i would like to thank Prof.dr. Fausto Gallucci for giving me an opportunity to work for this challenging project in the group of SPE-SIR group. His achievements have been always a true inspiration to me and his valuable guidance and support has been invaluable throughout this research.

I would like to thank my daily supervisor Dr.ing. Hamid Reza Godini for guiding me throughout this master project. I have gained a lot of experience in designing the *P&IDs*. I have experienced construction of an experimental setup and handling the lab equipment. Thanks a lot for identifying the mistakes and correcting me.

I would like to thank Erik Van Herk who helped me in constructing the experimental setup. He has helped me throughout the master project period either fixing the experimental setup or explaining the aspects of mechanical parts. I would like to thank Carlo Buijs for his support with the Mass Flow Controllers and safety aspects with the experimental setup. I would like to thank Ing. Peter Lipman who helped in logistics of cylinders and pressure regulators. I would always remember the effort Marlies Coolen Kuppens has done with installation of the Gas Chromatography. I would like to thank Ing. Paul Aendenroomer for constantly rectifying/solving the issues within the software and MFCs. Thanks to all technicians for supporting me during this masters thesis. I have gained a lot of knowledge with lab equipment.

I would like to thank the Phds, Vishnu Suresh kumar for his support during my master thesis and Arash Rahim Ali Mamaghani for providing the Gas Chromatography for this research. In addition, my sincere thanks to my colleague Sanjay Ramesh Kumar for his continuous support throughout this research and providing me catalysts for testing in the experimental setup. I enjoyed our discussions we had throughout this project period. I would like to thank Vishwanath Sastry, Harsh Gupta, Anirudh Prahlad and Ramya Tippireddy and all my other friends.

I would like to thank my parents, and my brother who kept supporting me constantly throughout my masters journey. It would not be possible for me to come all the way from my country for my masters without their constant support. I would like to dedicate my thesis to my family members who believed in me and encouraged me throughout my journey.



# Bibliography

- [1] I.E.Agency. CO<sub>2</sub> emission from fuel combustion, IECD/IEA, France. 2016. vii, 1, 2
- [2] Pen Chi Chiang and Shu Yuan Pan. Carbon dioxide mineralization and utilization. *Carbon Dioxide Mineralization and Utilization*, pages 1–452, 2017. vii, 4, 5
- [3] Francesco Dalena, Alessandro Senatore, Alessia Marino, Amalia Gordano, Marco Basile, and Angelo Basile. Chapter 1 - methanol production and applications: An overview. In Angelo Basile and Francesco Dalena, editors, *Methanol*, pages 3 – 28. Elsevier, 2018. vii, 7, 8, 9
- [4] Andrea Álvarez, Atul Bansode, Atsushi Urakawa, Anastasiya V. Bavykina, Tim A. Wezendonk, Michiel Makkee, Jorge Gascon, and Freek Kapteijn. Challenges in the greener production of formates/formic acid, methanol, and dme by heterogeneously catalyzed co<sub>2</sub> hydrogenation processes. *Chemical Reviews*, 117(14):9804–9838, 2017. vii, 10, 11
- [5] Huang X. Wang X. Wang X. Zhao, G. Progress in catalyst exploration for heterogeneous CO<sub>2</sub> reduction and utilization. *a critical review. J. Mater. Chem. A.*, pages 5(41), 21625–21649, 2017. 1
- [6] Nathan S. Lewis and Daniel G. Nocera. Powering the planet: Chemical challenges in solar energy utilization. *Proceedings of the National Academy of Sciences*, 103(43):15729–15735, 2006. 1
- [7] Broutin Paul Lebas Etienne Lecomte, Fabrice. *CO<sub>2</sub> Capture - Technologies to Reduce Greenhouse Gas Emissions*. Editions Technip, 2010. 1
- [8] J. Bruce H. Lee B.A. Callander E. Haites N. Harris K. Maskell (Eds.) J.T. Houghton, L.G.M. Filho. Climate change 1994. radiative forcing of climate change an evaluation of the ipcc is92 emission scenarios. *Cambridge Univ. Press*, 1995. 1
- [9] Scott C. Doney, Victoria J. Fabry, Richard A. Feely, and Joan A. Kleypas. Ocean acidification: The other co<sub>2</sub> problem. *Annual Review of Marine Science*, 1(1):169–192, 2009. 1
- [10] Adoption of the Paris Agreement. Paris Climate Change Conference; Paris, France. 2015. 1
- [11] C. Le Quere R.M. Andrew J.I. Korsbakken G.P. Peters N. Nakicenovic R. B. Jackson, J.G. Canadell. . *Nature Climate Change*, 6,, pages 7–10, 2015. 1
- [12] R. Lal D. A. N. Ussiri. Carbon Capture and Storage in Geologic Formations, Carbon Sequestration for Climate Change Mitigation and Adaptation. *Springer International Publishing, Cham.*, pages 497–545, 2017. 1
- [13] Peter M. Haugan and Helge Drange. Effects of co<sub>2</sub> on the ocean environment. *Energy Conversion and Management*, 37(6):1019 – 1022, 1996. Proceedings of the International Energy Agency Greenhouse Gases: Mitigation Options Conference. 1
- [14] T. Magnesen and T. Wahl. Biological impact of deep sea disposal of carbon dioxide. 1993. 1



- [15] N.Muradov. Liberating energy from carbon: introduction to decarbonization. *Energy Conversion and Management*, 22:22, 2014. 1
- [16] Bundit Limmeechokchai Tri Vicca Kusumadewi, Pornphimol Winyuchakrit. Long-term CO<sub>2</sub> Emission Reduction from Renewable Energy in Power Sector: The case of Thailand in 2050., *Energy Procedia*, pages 961–966, 2017. 2
- [17] Peter D. Cameron. The Revival of Nuclear Power: An Analysis of the Legal Implications. *Journal of Environmental Law*, 19(1):71–87, 01 2007. 2
- [18] S. Pacala and R. Socolow. Stabilization wedges: Solving the climate problem for the next 50 years with current technologies. *Science*, 305(5686):968–972, 2004. 2
- [19] Rezvani S. McIlveen-Wright D. Minchener A. Hewitt N. Huang, Y. Techno-economic study of CO<sub>2</sub> capture and storage in coal fired oxygen fed entrained flow IGCC power plants. *Fuel Processing Technology*, 89(9),, pages 916–925, 2008. 3
- [20] Anthony Ku, Parag Kulkarni, Roger Shisler, and Wei Wei. Membrane performance requirements for carbon dioxide capture using hydrogen-selective membranes in integrated gasification combined cycle (igcc) power plants. *Journal of Membrane Science*, 367:233–239, 02 2011. 3
- [21] Weirong Huang, Xiaobin Jiang, Gaohong He, Xuehua Ruan, Bo Chen, Aazad Khan Nizamani, Xiangcun Li, Xuemei Wu, and Wu Xiao. A novel process of h<sub>2</sub>/co<sub>2</sub> membrane separation of shifted syngas coupled with gasoil hydrogenation. *Processes*, 8(5):590, May 2020. 3
- [22] Edward Rubin, Hari Mantripragada, Aaron Marks, Peter Versteeg, and John Kitchin. The outlook for improved carbon capture technology. *Progress in Energy and Combustion Science*, 38:630–671, 10 2012. 3
- [23] Walter; Linssen-Jochen; Zapp Petra; Müller Thomas Markewitz, Peter; Leitner. Worldwide innovations in the development of carbon capture technologies and the utilization of CO<sub>2</sub>. *Energy Environmental Science*, 5(6),, pages 7281–7385, 2012. 3
- [24] Atul Bansode and Atsushi Urakawa. Towards full one-pass conversion of carbon dioxide to methanol and methanol-derived products. *Journal of Catalysis*, 309:66 – 70, 2014. 4, 10
- [25] A.G Fallis. *Strategic Energy Technology (SET) Plan*, volume 53. 2013. 4
- [26] Chunshan Song. *CO<sub>2</sub> Conversion and Utilization: An Overview*, chapter 1, pages 2–30. 4
- [27] M. Aresta and A. Dibenedetto. 14 - industrial utilization of carbon dioxide (co<sub>2</sub>). In M. Mercedes Maroto-Valer, editor, *Developments and Innovation in Carbon Dioxide (CO<sub>2</sub>) Capture and Storage Technology*, volume 2, pages 377 – 410. Woodhead Publishing, 2010. 4
- [28] M. Aresta. *Carbon Dioxide as Chemical Feedstock*. 01 edition, 2010. 5
- [29] Sebastian Verhelst, James Turner, L. Sileghem, and Jeroen Vancoillie. Methanol as a fuel for internal combustion engines. *Progress in Energy and Combustion Science*, 70:43–88, 01 2019. 5
- [30] The Methanol Industry Methanol Institue. <http://www.methanol.org/the-methanol-industry/>. 2017. 5, 7
- [31] Alain Goeppert Olah, George A. and N. Nakicenovic GK Surya Prakash, G.P. Peters. Chemical recycling of carbon dioxide to methanol and dimethyl ether: from greenhouse gas to renewable, environmentally carbon neutral fuels and synthetic hydrocarbons. *The Journal of organic chemistry*, 74.2., pages 487–498, 2008. 7

- [32] Kishore Natte, Helfried Neumann, Matthias Beller, and Rajenahally V. Jagadeesh. Transition-Metal-Catalyzed Utilization of Methanol as a C1 Source in Organic Synthesis. *Angewandte Chemie - International Edition*, 56(23):6384–6394, 2017. 7
- [33] Kenan Cem Tokay; Timur Dogu; Gulsen Dogu. Dimethyl ether synthesis over alumina based catalysts. *Chemical Engineering and Processing: Process Intensification*, (184):278–285, 2012. 8
- [34] Wei Hsin Chen, Bo Jhih Lin, How Ming Lee, and Men Han Huang. One-step synthesis of dimethyl ether from the gas mixture containing co2 with high space velocity. *Applied Energy*, 98:92–101, October 2012. 8
- [35] Zoha Azizi, Mohsen Rezaeimanesh, Tahere Tohidian, and Mohammad Reza Rahimpour. Dimethyl ether: A review of technologies and production challenges. *Chemical Engineering and Processing: Process Intensification*, 82:150 – 172, 2014. 8, 11
- [36] T.H. Fleisch, A. Basu, and R.A. Sills. Introduction and advancement of a new clean global fuel: The status of dme developments in china and beyond. *Journal of Natural Gas Science and Engineering*, 9:94 – 107, 2012. 8
- [37] <https://www.ceicdata.com/en/china/china-petroleum-chemical-industry-association-petrochemical-price-organic-chemical-material/cn-market-price-monthly-avg-organic-chemical-material-dimethyl-ether-990-or-above>. 8
- [38] Guangxin Jia, Yisheng Tan, and Yizhuo Han. A comparative study on the thermodynamics of dimethyl ether synthesis from co hydrogenation and co2 hydrogenation. *Industrial & Engineering Chemistry Research*, 45(3):1152–1159, 2006. 8
- [39] Rui-wen Liu, Zu-zeng Qin, Hong-bing Ji, and Tong-ming Su. Synthesis of dimethyl ether from co2 and h2 using a cu–fe–zr/hzsm-5 catalyst system. *Industrial & Engineering Chemistry Research*, 52(47):16648–16655, 2013. 8
- [40] L. Lloyd. Ammonia and Methanol Synthesis, in: Handbook of Industrial Catalysts,. *Springer US, Boston, MA*, pages 397–437, 2011. 8
- [41] B. M. Bhanage S. G. Jadhav, P.D. Vaidya and J. B. Joshi. Catalytic carbon dioxide hydrogenation to methanol: A review of recent studies. *Chemical Engineering Research and Design*, 92:2557, 2014. 9
- [42] G. A. Olah. Beyond oil and gas: The methanol economy. *Angewandte Chemie International Edition*, 44(18):2636–2639, 2005. 9
- [43] C. R. International. Curbing carbon emissions with green methanol. 2019. 9
- [44] Renata Jorge da Silva and Claudio J. A. Mota. 18. CO2 Hydrogenation to Methanol and Dimethyl Ether, pages 345 – 360. De Gruyter, Berlin, Boston, 31 Dec. 2019. 9
- [45] Jun Yoshihara and Charles T. Campbell. Methanol synthesis and reverse water–gas shift kinetics over cu(110) model catalysts: Structural sensitivity. *Journal of Catalysis*, 161(2):776 – 782, 1996. 10
- [46] Shaozhong Li, Yu Wang, Bin Yang, and Limin Guo. A highly active and selective mesostructured cu/alceo catalyst for co2 hydrogenation to methanol. *Applied Catalysis A: General*, 571:51 – 60, 2019. 10
- [47] Eun Jeong Choi, Yong Hee Lee, Dae-Won Lee, Dong-Ju Moon, and Kwan-Young Lee. Hydrogenation of co2 to methanol over pd–cu/ceo2 catalysts. *Molecular Catalysis*, 434:146 – 153, 2017. 10

- [48] Jong-Wook Bae, H. S. Potdar, Suk-Hwan Kang, and Ki-Won Jun. Coproduction of methanol and dimethyl ether from biomass-derived syngas on a  $\text{CuZnO}/\text{Al}_2\text{O}_3$  hybrid catalyst. *Energy & Fuels*, 22(1):223–230, 2008. 10
- [49] Hamid Reza Godini, Mohammadali Khadivi, Mohammadreza Azadi, Oliver Görke, Seyed Mahdi Jazayeri, Lukas Thum, Reinhard Schomäcker, Günter Wozny, and Jens-Uwe Repke. Multi-scale analysis of integrated  $\text{CH}_4$  and  $\text{CO}_2$  utilization catalytic processes: Impacts of catalysts characteristics up to industrial-scale process flowsheeting, part i: Experimental analysis of catalytic low-pressure  $\text{CO}_2$  to methanol conversion. *Catalysts*, 10(5):505, May 2020. 10, 13, 32, 36
- [50] Xin-Mei Liu, G. Q. Lu, Zi-Feng Yan, and Jorge Beltramini. Recent advances in catalysts for methanol synthesis via hydrogenation of  $\text{CO}$  and  $\text{CO}_2$ . *Industrial & Engineering Chemistry Research*, 42(25):6518–6530, 2003. 10
- [51] Fereydoon Yaripour, F. Baghaei, I. Schmidt, and J. Perregaard. Catalytic dehydration of methanol to dimethyl ether (dme) over solid-acid catalysts. *Catalysis Communications*, 6:147–152, 02 2005. 11
- [52] Zahra Hosseini, Majid Taghizadeh, and Fereydoon Yaripour. Synthesis of nanocrystalline  $\text{Al}_2\text{O}_3$  by sol-gel and precipitation methods for methanol dehydration to dimethyl ether. *Journal of Natural Gas Chemistry - J NAT GAS CHEM*, 20:128–134, 03 2011. 11
- [53] Optimization of hydrothermal synthesis of  $\text{H-ZSM-5}$  zeolite for dehydration of methanol to dimethyl ether using full factorial design. *Journal of Natural Gas Chemistry*, 21(3):344 – 351, 2012. 11
- [54] Andrés García-Trenco and Agustín Martínez. Direct synthesis of dme from syngas on hybrid  $\text{CuZn}/\text{ZSM-5}$  catalysts: New insights into the role of zeolite acidity. *Applied Catalysis A: General*, 411-412:170 – 179, 2012. 12
- [55] Qi Yang, Meng Kong, Zheyong Fan, Xiangju Meng, Jinhua Fei, and Feng-Shou Xiao. Aluminum fluoride modified  $\text{H-ZSM-5}$  zeolite with superior performance in synthesis of dimethyl ether from methanol. *Energy & Fuels*, 26(7):4475–4480, 2012. 12
- [56] Kevin McBride, Thomas Turek, and Robert Güttel. Direct dimethyl ether synthesis by spatial patterned catalyst arrangement: A modeling and simulation study. *AIChE Journal*, 58(11):3468–3473, 2012. 12, 34
- [57] G. Bonura, M. Cordaro, C. Cannilla, A. Mezzapica, L. Spadaro, F. Arena, and F. Frusteri. Catalytic behaviour of a bifunctional system for the one step synthesis of DME by  $\text{CO}_2$  hydrogenation. *Catalysis Today*, 228:51–57, 2014. 12
- [58] Shoujie Ren, Weston R. Shoemaker, Xiaofeng Wang, Zeyu Shang, Naomi Klinghoffer, Shiguang Li, Miao Yu, Xiaoqing He, Tommi A. White, and Xinhua Liang. Highly active and selective  $\text{Cu-ZnO}$  based catalyst for methanol and dimethyl ether synthesis via  $\text{CO}_2$  hydrogenation. *Fuel*, 239(November 2018):1125–1133, 2019. 12
- [59] F. Frusteri, G. Bonura, C. Cannilla, G. Drago Ferrante, A. Aloise, E. Catizzzone, M. Migliori, and G. Giordano. Stepwise tuning of metal-oxide and acid sites of  $\text{CuZnZr-MFI}$  hybrid catalysts for the direct DME synthesis by  $\text{CO}_2$  hydrogenation. *Applied Catalysis B: Environmental*, 176-177:522–531, 2015. 12
- [60] G. Bonura, C. Cannilla, L. Frusteri, A. Mezzapica, and F. Frusteri. DME production by  $\text{CO}_2$  hydrogenation: Key factors affecting the behaviour of  $\text{CuZnZr}$ /ferrierite catalysts. *Catalysis Today*, 281:337–344, 2017. 12, 57

- 
- [61] Zhuangdian Liang, Peng Gao, Zhiyong Tang, Min Lv, and Yuhan Sun. Three dimensional porous cu-zn/al foam monolithic catalyst for co<sub>2</sub> hydrogenation to methanol in microreactor. *Journal of CO<sub>2</sub> Utilization*, 21:191–199, 10 2017. 13
- [62] Fausto Gallucci, Luca Paturzo, and Angelo Basile. An experimental study of co<sub>2</sub> hydrogenation into methanol involving a zeolite membrane reactor. *Chemical Engineering and Processing: Process Intensification*, 43(8):1029 – 1036, 2004. 13, 14, 32
- [63] Weijie Cai, Pilar Ramirez de la Piscina, Jamil Toyir, and Narcis Homs. Co<sub>2</sub> hydrogenation to methanol over cuznga catalysts prepared using microwave-assisted methods. *Catalysis Today*, 242:193 – 199, 2015. Fuel roadmap for the mid-21st century: Advanced catalytic processes and strategies for the production and use of energy and fuels. 13
- [64] Kalala Jalama. Carbon dioxide hydrogenation over nickel-, ruthenium-, and copper-based catalysts: Review of kinetics and mechanism. *Catalysis Reviews*, 59(2):95–164, 2017. 13
- [65] Danjun WANG, Furong TAO, Huahua ZHAO, Huanling SONG, and Lingjun CHOU. Preparation of cu/zno/al<sub>2</sub>o<sub>3</sub> catalyst for co<sub>2</sub> hydrogenation to methanol by co<sub>2</sub> assisted aging. *Chinese Journal of Catalysis*, 32(9):1452–1456, 2011. 13
- [66] Rohit Gaikwad, Atul Bansode, and Atsushi Urakawa. High-pressure advantages in stoichiometric hydrogenation of carbon dioxide to methanol. *Journal of Catalysis*, 343:127–132, 2016. 13
- [67] Javier Ereña, Irene Sierra, Martin Olazar, Ana G. Gayubo, and Andrés T. Aguayo. Deactivation of a cuoznoal<sub>2</sub>o<sub>3</sub>/al<sub>2</sub>o<sub>3</sub> catalyst in the synthesis of dimethyl ether. *Industrial & Engineering Chemistry Research*, 47(7):2238–2247, 2008. 13
- [68] Fei Zha, Haifeng Tian, Jun Yan, and Yue Chang. Multi-walled carbon nanotubes as catalyst promoter for dimethyl ether synthesis from co<sub>2</sub> hydrogenation. *Applied Surface Science*, 285:945–951, 2013. 13
- [69] Xinhui Zhou, Tongming Su, Yuexiu Jiang, Zuzeng Qin, Hongbing Ji, and Zhanhu Guo. Cu-*fe*<sub>2</sub>o<sub>3</sub>-*ceo*<sub>2</sub>/hzsm-5 bifunctional catalyst hydrogenated co<sub>2</sub> for enhanced dimethyl ether synthesis. *Chemical Engineering Science*, 153:10–20, 2016. 13, 33
- [70] Kaisar Ahmad and Sreedevi Upadhyayula. Greenhouse gas co<sub>2</sub> hydrogenation to fuels: A thermodynamic analysis. *Environmental Progress & Sustainable Energy*, 38(1):98–111, 2019. 14
- [71] J. Skrzypek, M. Lachowska, M. Grzesik, J. TBoczyDski, and P. Nowak. Thermodynamics and kinetics of low pressure methanol synthesis. *The Chemical Engineering Journal and The Biochemical Engineering Journal*, 58:101–108, 1995. 16
- [72] Francesco Arena, Katia Barbera, Giuseppe Italiano, Giuseppe Bonura, Lorenzo Spadaro, and Francesco Frusteri. Synthesis, characterization and activity pattern of cu-zno/zro<sub>2</sub> catalysts in the hydrogenation of carbon dioxide to methanol. *Journal of Catalysis*, 249(2):185–194, 2007. 32
- [73] Marina Bukhtiyarova, Thomas Lunkenbein, Kevin Kähler, and Robert Schlögl. Methanol Synthesis from Industrial CO<sub>2</sub> Sources: A Contribution to Chemical Energy Conversion. *Catalysis Letters*, 147(2):416–427, feb 2017. 32, 36
- [74] Xinhui Zhou, Tongming Su, Yuexiu Jiang, Zuzeng Qin, Hongbing Ji, and Zhanhu Guo. Cu-*fe*<sub>2</sub>o<sub>3</sub>-*ceo*<sub>2</sub>/hzsm-5 bifunctional catalyst hydrogenated co<sub>2</sub> for enhanced dimethyl ether synthesis. *Chemical Engineering Science*, 153:10–20, 2016. 36



## Appendix A

# Catalyst abbreviations, Composition

Table A.1: Catalyst abbreviation used in this research study

S.no	Catalysts synthesized/procured	Abbreviation
1	Co-Precipitation catalyst	CP single catalyst/ Co-Preci
2	Precipitation-Impregnation catalyst	PI single catalyst
3	Copper based methanol synthesis catalyst	LPCC
4	Co-Precipitation catalyst with HZSM-5	CP dual catalyst
5	Co-Impregnation catalyst with HZSM-5	CI dual catalyst/CI
6	Zeolite HZSM-5 (Si/Al = 30)	HZSM-5

Table A.2: Composition by weight percentage present in the single catalysts

S.no	Single catalysts	CuO (wt%)	ZnO (wt%)	$Al_2O_3$ (wt%)	MgO (wt%)	Carbon (wt%)
1	CP single catalyst	50	50	-	-	-
2	PI single catalyst	30	70	-	-	-
3	LPCC	63.5	25	10	1.5	-

Table A.3: Composition by weight percentage present in the dual catalysts

S.no	Dual catalysts	CuO (wt %)	ZnO (wt %)	H-ZSM5 (wt %)
1	CI dual catalyst	16.65	16.65	66.66

## Appendix B

# GC Calibration

A GC Calibration is a crucial step that needs to be performed to know the concentration of the components that are obtained from the reactions that takes places in the reactor. In order to get the calibration curves 6 various cylinders with different composition of gases mentioned in table B.1 were injected into the Gas Chromatograph (GC). A clear schematic of the Gas chromatograph used for this research is shown in figure B.1. The gases that can be detected in the GC is based on the type of the column. Therefore, the information related to the columns and the respective gases that can be detected is shown in the table B.2. The calibration that is carried out using the gas cylinders with varied composition the calibrations curves for the gases are shown in the fig B.2 With reference to these Calibration curves and peak area the composition of the products were identified. The outlet gases composition from the Titanium reactor was injected into the GC. The 4 channels that were present in the GC as shown in below table helps in identifying this composition.

The Co-Precipitation catalyst exhibited a carbon balance of  $100 \pm 5$ . Utilizing the same catalyst with commercial HZSM-5 catalyst didn't result in any new compounds in the GC except DME. Hence, the DME reported in the bed configurations and Dual catalyst was calculated based on the Carbon Balance.

Table B.1: Gas cylinders used for GC Calibration

Cylinder	Gases	Composition (%)
1	Carbondioxide	0.692
	Hydrogen	1.5
	Nitrogen	17.9
	Argon	Rest
2	Methane	9.09
	Hydrogen	13
	Carbon monoxide	15.9
	Argon	Rest
3	Propane	0.997
	Propylene	0.991
	Ethane	0.997
	Carbon-dioxide	5.00
	Oxygen	0.537
	Methane	0.954
	Ethylene	0.960
	Carbon monoxide	5.01
	Nitrogen	4.999
	Helium	Rest
4	Propane	1.994
	Propylene	1.981
	Ethane	1.981
	Carbon-dioxide	1.995
	Methane	1.885
	Ethylene	1.957
	Hydrogen	2.020
	Carbon monoxide	2.003
Nitrogen	2.038	
	Argon	Rest

Table B.2: Characteristics of Compact GC

Channel	Gases detected	Detector	Columns
1	Methanol, DME	TCD	MXT-624 3.0um 15m×0.53mm
2	Carbon-dioxide, Water	TCD	Rt-UBond 3m×0.32mm and Rt-UBond 12m×0.32mm
3	Nitrogen, Methane, Carbon monoxide,	TCD	Rt-QBond 3m×0.32mm and Molsieve 5A 7m×0.32mm
4	Hydrogen	TCD	Rt-QBond 3m×0.32mm and Molsieve 5A 7m×0.32mm



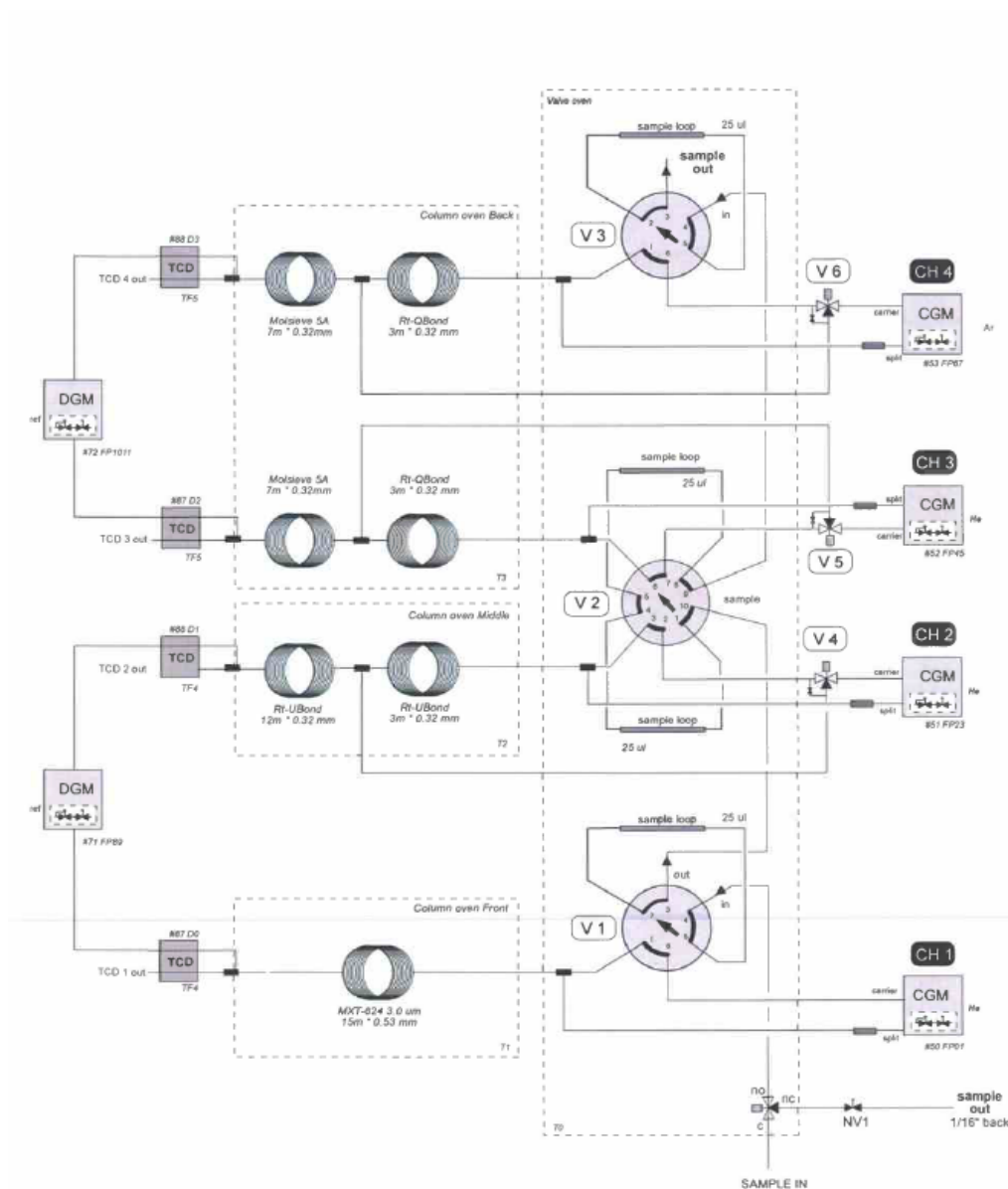


Figure B.1: Schematic Representation of GC

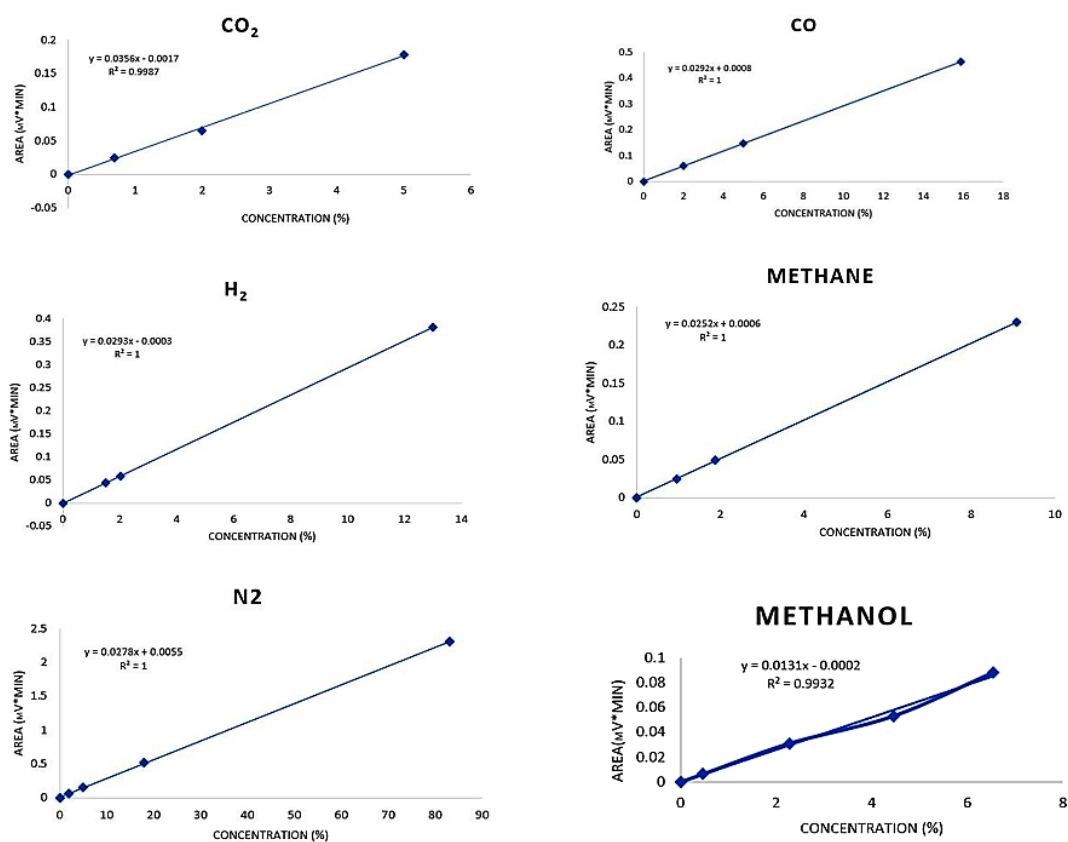


Figure B.2: Calibration curves for gas components based on GC analysis

# Appendix C

## Piping and Instrumentation Diagram (P&ID)

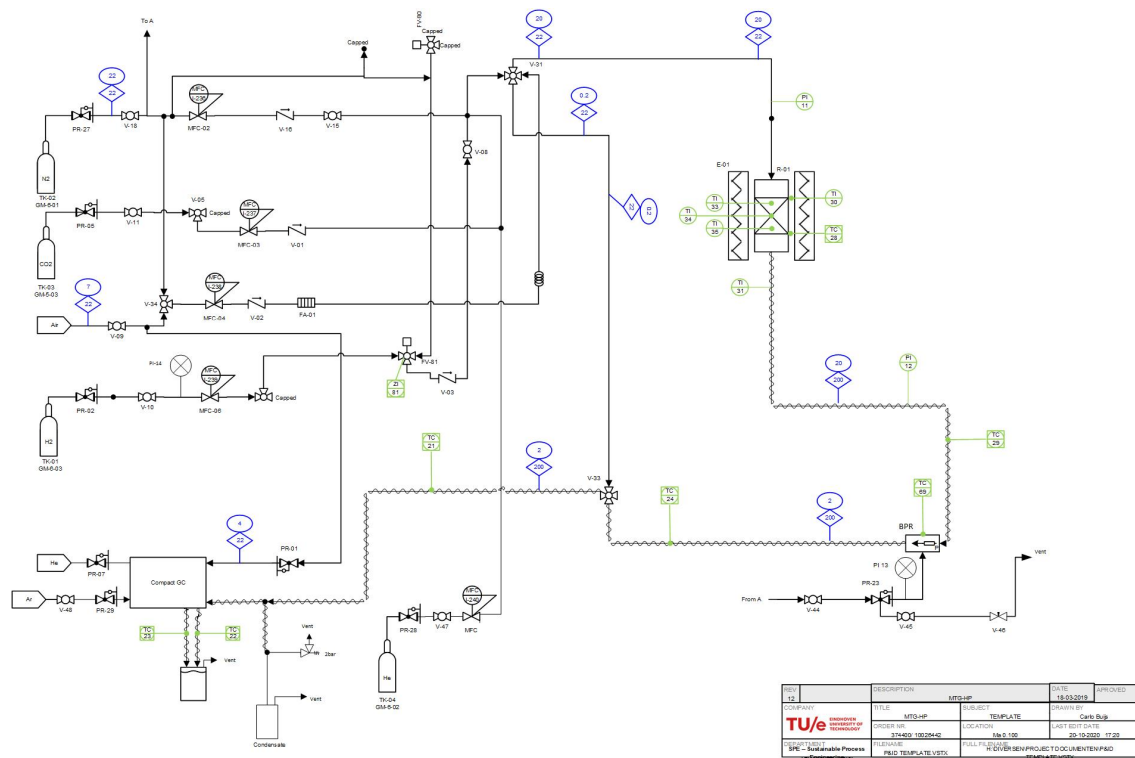


Figure C.1: Piping and Instrumentation Diagram(P&ID) of the experimental setup

# Appendix D

## Dual Catalyst

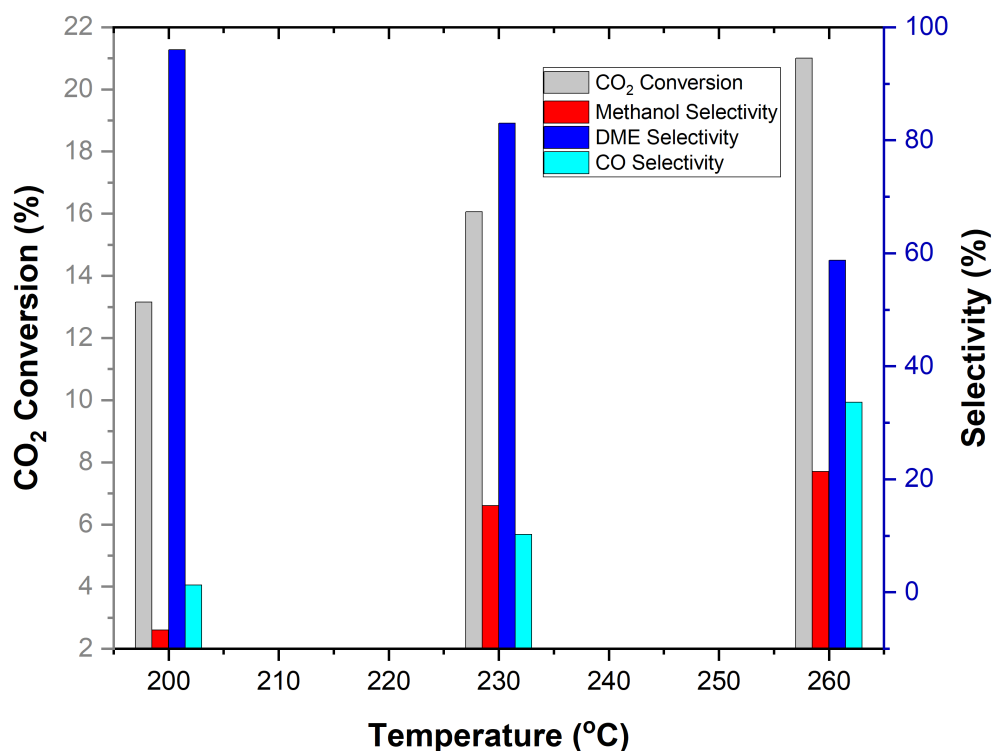


Figure D.1: Effect of temperature on  $CO_2$  Conversion and Selectivity of Methanol, DME, and CO

The figure D.1 shows the conversion of the carbon dioxide for  $CO_2$  hydrogenation to DME on the CuO-ZnO/HZSM-5 Co-impregnated dual catalyst under 15 bar pressure with varied temperature ranging from 200°C to 260°C. The figure illustrates that the conversion of  $CO_2$  increases with elevation of temperatures. It can be observed that the conversion has increased from 13% to 21% when the temperature rose from 200°C to 260°C. An increasing trend can be seen with Methanol Selectivity and CO selectivity with increase in the temperature. Besides, a DME selectivity decreased while the temperature was increased. The same trends of  $CO_2$  conversion, Selectivity of DME were observed in the literature for a oxalate-FER/2 dual catalyst [60].

### D.0.1 Sensitivity analysis

Table D.1: Calculations reported for the dual Co-Impregnated Dual catalyst

TC	Methanol +DME yield	Methanol +DME yield rep	Column-1	Column-2	Column-3
1	12.27	13.55	26.56	50.89	101.17
a	14.28	14.51	24.32	50.28	8.07
b	10.96	11.85	26.43	4.39	-4.82
ab	13.35	12.81	323.84	3.67	-2.21
c	11.64	16.65	2.00	-2.23	-0.6
ac	14.78	14.61	2.38	-2.59	-0.72
bc	11.65	9.45	3.13	0.37	-0.35
abc	12.19	11.96	0.54	-2.5	-2.97

The design of experiments as mentioned in 4.1 are conducted twice in the fixed bed reactor and are reported here. The Column 1, Column 2, Column 3 reported here are calculated using the Table D.2.

Table D.2: Analysis used for identifying the predominant parameter

TC	Column 1	Column 2	Column 3
1	1+a	1+a+b+ab	1+a+b+ab+c+ac+bc+abc
a	b+ab	c+ac+bc+abc	a-1+ab-b+ac-c+abc-bc
b	c+ac	a-1+ab-b	b+ab-1-a+bc+abc-c-ac
ab	bc+abc	ac-c+abc-bc	ab-b-a+1+abc-bc-ac+c
c	a-1	b+ab-1-a	c+ac+bc+abc-1-a-b-ab
ac	ab-b	bc+abc-c-ac	ac-c+abc-bc-a+1-ab+b
bc	ac-c	ab-b-1+1	bc+abc-c-ac-b-ab+1+a
abc	abc-bc	abc-bc-ac+c	abc-bc-ac+c-ab+b+a-1

Symbol	Description	Unit
Cb	Catalytic bed	
GHSV	Gas Hourly Space Velocity	$\text{h}^{-1}$
P	Pressure	bar
T	Temperature	$^{\circ}\text{C}$
$Q_{TOTAL}$	Total Flow rate	$\text{ml}_n/\text{min}$
$X_{CO_2}$	Conversion of Carbon dioxide	%
x	Mol fraction	
$T_a$	Ambient Temperature	$^{\circ}\text{C}$
n	Molar Flow rate	$\text{mol}/\text{min}$

Table D.3: Nomenclature